Proton-neutron pairing in $Z=N$ nuclei with $A=76-96$

Alan L. Goodman

Department of Physics, Tulane University, New Orleans, Louisiana 70118
(Received 29 December 1998; published 16 June 1999)

The ground states of even-even $Z=N$ nuclei are determined with the isospin generalized BCS equations and the HFB equation. The calculations permit the simultaneous existence of the following Cooper pairs: pp, nn, $pn(T=1)$, and $pn(T=0)$ where the two nucleons in a pair occupy space-spin orbitals which are related by time reversal, as well as $pn(T=0)$ where the two nucleons are in identical space-spin orbitals. There is a transition from $T=1$ Cooper pairs at the beginning of this isotope sequence to $T=0$ Cooper pairs at the end of the sequence. Near the middle of the isotope sequence, there is coexistence of a $T=0$ pair superfluid and a $T=1$ pair superfluid in the same wave function. The fluctuation in the particle number is reduced if the wave function contains proton-neutron pairing. The fluctuation in the isospin is eliminated and isospin is conserved if the wave function contains only $T=0$ pairing. [S0556-2813(99)05407-2]

PACS number(s): 21.60.−n

I. INTRODUCTION

During the past few years there has been a rebirth of interest in proton-neutron pair correlations. There are several reasons for this renaissance. (1) Radioactive nuclear beams have now extended the $N=Z$ line up to ^{100}Sn [1,2]. In $N=Z$ nuclei, protons and neutrons occupy the same spatial orbitals and have maximum spatial overlap. Therefore $N=Z$ nuclei provide the best conditions for finding pn pair correlations. It is now possible to study pn pairing in medium-mass nuclei. (2) The new generation of 4π detectors is providing experimental data which was not available in previous decades. (3) There is considerable interest in determining the location of the proton drip line in medium-mass nuclei [3–6]. The proton drip line is close to the $N=Z$ line. In these nuclei pn pairing might create additional binding energy, and provide stability to some nuclei which would otherwise be unstable. Therefore pn pairing could alter the location of the proton drip line. (4) pn pairing is expected to play a significant role in β decay [7–9]. Neutrinoless double β decay has fundamental significance in elementary particle physics.

The initial theory of nucleon pair correlations included Cooper pairs which contain two protons or two neutrons [10,11]. It did not include Cooper pairs containing one proton and one neutron. In this BCS approximation, the quasiparticle operators are defined by a 2×2 unitary transformation of the particle operators. In the early 1960's it was recognized that this pairing theory was incomplete, and that it needed to be generalized to include proton-neutron Cooper pairs [12]. This generalization occurred during the period 1964–1972, and it proceeded in several steps [13–23]. (1) The BCS theory was generalized to include $p\bar{p}$, $n\bar{n}$, and $p\bar{n}$ Cooper pairs, where the bar indicates that the second nucleon in a pair occupies a space-spin orbital which is the time-reverse of the first nucleon's orbital, and the two nucleons are coupled to isospin $T=1$ [14,16,17]. (2) A BCS theory was obtained for $p\bar{n}$ Cooper pairs, where the two nucleons are coupled to $T=0$ [15]. (3) A unified BCS theory was derived for $p\bar{p}$, $n\bar{n}$, and $p\bar{n}$ Cooper pairs, which includes both $T=0$ and $T=1$ $p\bar{n}$ pairs [18–20]. In this theory the quasiparticle operators are defined by a 4×4 unitary transformation of the particle operators, and the two nucleons in a pair occupy orbitals related by time reversal. (4) However, the Pauli exclusion principle does not prevent a proton and a neutron from occupying the *same* space-spin orbital and forming a pn Cooper pair, if they are coupled to $T=0$. (Hereafter, pn refers to this particular pair, and not to $p\bar{n}$ pairs.) There is an isospin-generalized BCS theory which includes pn ($T=0$) Cooper pairs, as well as $p\bar{p}$, $n\bar{n}$, and $p\bar{n}$ ($T=0$ and $T=1$) Cooper pairs [23]. In this theory the quasiparticle operators are defined by an 8×8 unitary transformation of the particle operators.

From 1967–1970 the isospin generalized BCS theory and the HFB theory were used to calculate the ground states of even $N=Z$ nuclei in the sd shell [19–23]. For these nuclei $T=0$ proton-neutron pairing correlations are much stronger than proton-proton and neutron-neutron pairing correlations. The $T=0$ pairing significantly alters the ground state properties of some of these nuclei. Subsequent calculations [24–30] investigated the ground states of $N=Z$ nuclei in the pf shell and $N\neq Z$ nuclei in the sd and pf shells. This early work is reviewed in Ref. [13]. From 1978–1982 HFB cranking calculations [31–33] investigated the effect of rotation on proton-neutron pairing. They demonstrated that pn pairing is much more persistent in the presence of rotation than are the usual $p\bar{p}$ and $n\bar{n}$ pairs. Consequently a ground band with $T=1$ pairing could be crossed by another band with $T=0$ pairing at a critical spin [32,33]. In 1983 the finite-temperature HFB cranking theory [34,35] was used to determine the effect of temperature on proton-neutron pairing [36–38]. The result was that the higher multipoles ($J>0$) of the pair field Δ are more resistant against increasing temperature than the standard monopole ($J=0$, $T=1$) pair field. Including Cooper pairs with all possible values of JT more than doubles the critical temperature for the disappearance of pairing.

Recently there have been many articles devoted to proton-neutron pairing [7,8,39–60]. An experiment on the $N=Z$ even-even nucleus ^{74}Rb finds that the $T=1$ ground band is

crossed by a $T=0$ band at a critical spin [44]. This has been interpreted as the crossing of a band with $T=1$ pairing by a band with $T=0$ pairing [44,50]. Other calculations find that $T=0$ pairing is crucial for determining the crossing frequency ω_c for such band crossings [58]. The influence of proton-neutron correlations on back bending has been investigated [41,42]. HFB calculations on ^{48}Cr find that $T=0$ pairing has a dramatic effect upon the deformation at high spins [57]. Shell model Monte Carlo calculations in the pf shell find that $T=0$ proton-neutron correlations persist to higher temperatures than the correlations between like nucleons [47–50]. This has a significant effect upon the temperature dependence of the Gamow-Teller strength [48]. EXCITED VAMPIR calculations for $N=Z$ even nuclei with $A=72–84$ find that $T=0$ and $T=1$ proton-neutron pairing both make a significant contribution to the pairing energy [43]. Some articles have considered simple model Hamiltonians in order to compare the isospin generalized BCS approximation with exact results [51–55]. For example, calculations for the SO(8) model find that the BCS energies are in good agreement with the exact energies [52].

The purpose of this article is to investigate proton-neutron pair correlations in $N=Z$ even nuclei with $A=76–96$. The calculations include all of the pair modes discussed above, i.e., $p\bar{p}$, $n\bar{n}$, $p\bar{n}$ ($T=0$ and $T=1$), and pn ($T=0$), as well as the time reverse of these proton-neutron pairs. There is a competition between these different pair modes, and a competition between $T=0$ pairing and $T=1$ pairing. Calculations will be performed using the isospin generalized BCS theory and the HFB theory. These theories permit the simultaneous coexistence of all pair modes in the same wave function. However, since these theories are derived from a variational principle, in a specific case it may be energetically favorable for all of the occupation probability to be placed in one particular pair mode. In other cases it may be energetically favorable to have more than one pair mode coexist in the same wave function. For the nuclei considered here, will the $T=0$ pair modes and the $T=1$ pair modes be mutually exclusive, or will $T=0$ pairing and $T=1$ pairing peacefully coexist in the same wave function? The HFB theory treats pairing and deformation simultaneously and self-consistently. Therefore these calculations can show how proton-neutron pairing affects the deformation, and vice versa.

II. HAMILTONIAN

The model space includes the $2p_{1/2}$, $2p_{3/2}$, $1f_{5/2}$, and $1g_{9/2}$ shells. A closed core of $^{56}_{28}\text{Ni}_{28}$ is assumed. This model space was used in shell model Monte Carlo calculations for ^{74}Rb [50] and in HFB calculations for Sr, Zr, and Mo isotopes [61].

The Hamiltonian is

$$H = \sum_j e_j C_j^\dagger C_j + \frac{1}{4} \sum_{ijkl} \langle ij|v_a|kl\rangle C_i^\dagger C_j^\dagger C_l C_k, \quad (2.1)$$

where e_j is the single-particle energy, v_a is the antisymmetrized effective interaction, and $|i\rangle$ denotes $|nljm\tau\rangle$, where τ

TABLE I. Single-particle energies e_j.

Orbital	$e_j(^{57}\text{Ni})$ (MeV)	$e_j(\text{Nilsson})$ (MeV)	$e_j(\text{KFP})$ (MeV)
$2p_{1/2}$	1.113	2.432	0.690
$2p_{3/2}$	0.000	2.261	0.000
$1f_{5/2}$	0.769	0.000	−0.140
$1g_{9/2}$	3.000	4.178	1.580

is p or n. The effective interaction was calculated by Kuo from the Paris potential. The monopole terms were modified by Nowacki to provide a good fit to the spectra of the Ni isotopes [62].

There have been extensive efforts to determine the deformation of ^{80}Zr [43,61,63–76]. It was found that the ground state shape is extremely sensitive to the choice of the parameters in the Hamiltonian [67,72,74]. Small changes in these parameters create large changes in the equilibrium shape. Similarly, small changes in the Fermi energy or orbital occupation probabilities cause large alterations in the shape. For these reasons, we use three different choices for the single-particle energies e_j, which are given in Table I. All calculations will be repeated for each of these three choices. The purpose is to determine how the pair gaps and shapes depend upon the choice of single-particle energies. Will the pairing properties be as sensitive to this choice as are the deformation properties? Does the competition between $T=0$ pairing and $T=1$ pairing depend upon this choice? Sections III B and III C provide additional reasons why more than one choice for e_j is considered. The first choice for the energies e_j is taken from the experimental spectrum of ^{57}Ni, and will be referred to as $e_j(^{57}\text{Ni})$. These energies were also used in the shell model Monte Carlo calculations for ^{74}Rb [50]. The second choice for the energies e_j, referred to as $e_j(\text{Nilsson})$, is determined by requiring that the Hartree-Fock spherical single-particle energies for ^{80}Zr are equal to the Nilsson spherical single-particle energies for ^{80}Zr. The rationale for this prescription and the equation used to determine $e_j(\text{Nilsson})$ are given in Sec. III B. The third choice for the energies e_j is taken from Table II in Ref. [61], which uses HFB in the same model space, and determines e_j from experimental spectra in the $A \approx 90$ mass region. This will be referred to as $e_j(\text{KFP})$.

III. HARTREE-FOCK

Solutions to the Hartree-Fock (HF) equation will be obtained. The HF wave functions serve several purposes. (1) The HF single-particle orbitals will be used as the basis states for finding the solutions of the isospin generalized BCS equations. (2) The HF solutions corresponding to spherical shapes will be used to examine how the energies of the j shells vary with mass number. (3) The HF states will be used for a preliminary evaluation of the dependence of the deformation on the choice of the single-particle energies e_j.

A. Theory

The HF eigenvalue equation is

$$h|\alpha\rangle = \epsilon_\alpha|\alpha\rangle. \tag{3.1}$$

The HF Hamiltonian h is

$$h = e + \mathcal{U}, \tag{3.2}$$

where e is the single-particle energy and $\mathcal{U}$ is the HF potential

$$\mathcal{U}_{ij} = \sum_{\alpha\text{occ}} \langle i\alpha|v_a|j\alpha\rangle, \tag{3.3}$$

where the sum is on the occupied orbitals. Equations (3.1)–(3.3) are solved by iteration to obtain the self-consistent HF single-particle orbitals

$$|\alpha\rangle = \sum_i D_{\alpha i}|i\rangle, \tag{3.4}$$

and the HF single-particle energies

$$\epsilon_\alpha = \langle\alpha|e|\alpha\rangle + \sum_{\beta\text{occ}} \langle\alpha\beta|v_a|\alpha\beta\rangle. \tag{3.5}$$

The energy of the nucleus $E_{\text{HF}} = \langle H\rangle$ is evaluated using the HF wave function. In the notation above $|\alpha\rangle$ and $|i\rangle$ include all nucleon quantum numbers, including the isospin (p or n). In the remainder of the article, $|\alpha\rangle$ denotes the space-spin component of the orbital, but not the isospin component. For an $N=Z$ even nucleus, the nucleon orbitals occur in degenerate quartets $|\alpha p\rangle$, $|\alpha n\rangle$, $|\bar\alpha p\rangle$, and $|\bar\alpha n\rangle$, where $|\bar\alpha\rangle$ is the time reverse of $|\alpha\rangle$. The orbital $|\alpha\rangle$ is composed of basis states $|i\rangle$ which have $m-1/2$ equal to an even integer.

B. Spherical single-particle energies

For some isotopes the HF equation has a spherically symmetric solution, where the deformation $\beta=0$ and the HF orbitals are $|\alpha\rangle = |nljm\rangle$. In these wave functions a particular set of j shells is completely filled, while the remaining j shells are empty. Also, the energies ϵ_j of the empty shells must be greater than the energies of the filled shells. (Inverted states, where an empty shell is below a filled shell, do not qualify.) These spherical states are only possible for particular values of Z and N. Except at magic numbers, the energies E_{HF} for these spherical HF states are usually greater than the energies of deformed HF states.

Figure 1 shows the HF single-particle energies ϵ_j for the spherical HF solutions. This calculation uses the single-particle energies $e_j(^{57}\text{Ni})$, which at first appear to be the natural choice for e_j. In ^{68}Se the $2p_{1/2}$ and $2p_{3/2}$ shells are full. In ^{80}Zr the $2p_{1/2}$, $2p_{3/2}$, and $1f_{5/2}$ shells are full. In ^{100}Sn all shells are full. Observe that the ordering of the energies ϵ_j is very mass dependent. There are crossings in the energies of the j shells as the mass number varies. These crossings are caused by the monopole component of the effective interaction. Observe that the ordering in ^{57}Ni is very
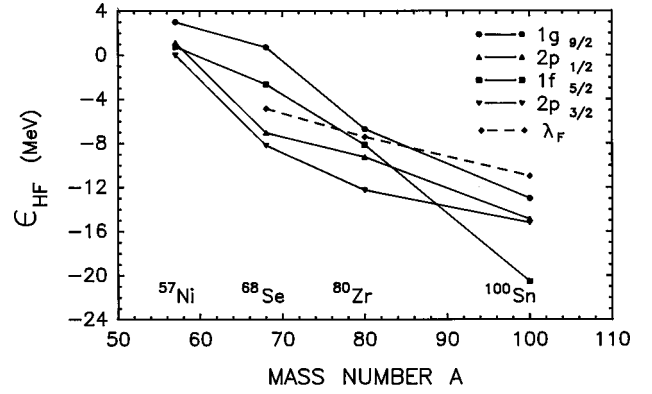

FIG. 1. Spherical Hartree-Fock single-particle energies ϵ_j versus mass number A. The energies $e_j(^{57}\text{Ni})$ are used.

different than the ordering in ^{100}Sn. Most notably, in ^{100}Sn the $1f_{5/2}$ shell falls below the other shells. How does this compare with experiment? For the $1f_{5/2}$, $2p_{3/2}$, $2p_{1/2}$, and $1g_{9/2}$ shells in ^{100}Sn, the HF energies ϵ_j are 0, 5.33, 5.65, and 7.55 MeV, whereas the experimental energies are 0, 2.33, 5.18, and 5.79 MeV [2]. (The energies are shifted by a constant, so that the lowest energy is 0.) Notice that theory and experiment have the j shells ordered in the same sequence in ^{100}Sn. However there are quantitative differences between the two spectra.

In the mass region around ^{80}Zr, the deformation can be very sensitive to the spherical energies ϵ_j. Because the monopole effective interaction causes the energies ϵ_j to be so mass dependent, and the monopole interaction has been adjusted to fit Ni spectra and not $A=76-96$ spectra, it follows that selecting the energies e_j from the ^{57}Ni experimental spectrum might not be the best choice for e_j. To improve the likelihood that the theoretical ordering of the j shells closely resembles the experimental ordering for the $A=76-96$ mass region, it may be desirable to choose the energies e_j so that the HF spherical energies for ^{80}Zr are equal to the Nilsson spherical energies

$$\epsilon_j(\text{HF}, {}^{80}\text{Zr}, \beta=0) = e_j + \mathcal{U}_j(\text{HF}, {}^{80}\text{Zr}, \beta=0)$$

$$= \epsilon_j(\text{Nilsson}, \beta=0). \tag{3.6}$$

For spherical HF states, $\mathcal{U}_{ij}$ is diagonal, so that $\mathcal{U}_j = \mathcal{U}_{jj}$. The spherical Nilsson energies are taken from a Nilsson diagram specifically constructed to fit ^{80}Zr [67]. The isotope ^{80}Zr is selected for this procedure because it is the only $N=Z$ even isotope in the $A=76-96$ mass region which has a spherical HF solution. Equation (3.6) is used to determine the energies e_j, which are given as $e_j(\text{Nilsson})$ in Table I. These energies are shifted by a constant, so that the lowest energy is zero.

The deformation and pairing properties of a particular nucleus are determined, in part, by the energies ϵ_j. So it is then useful to compare the energies ϵ_j resulting from the three choices of e_j given in Table I. Figure 2 shows the spherical Hartree-Fock energies ϵ_j for ^{80}Zr. The energies ϵ_j are shifted so that the lowest energy is 0. The $e_j(\text{KFP})$ spectrum is compressed relative to the $e_j(^{57}\text{Ni})$ spectrum. However the two spectra have the levels in the same order with
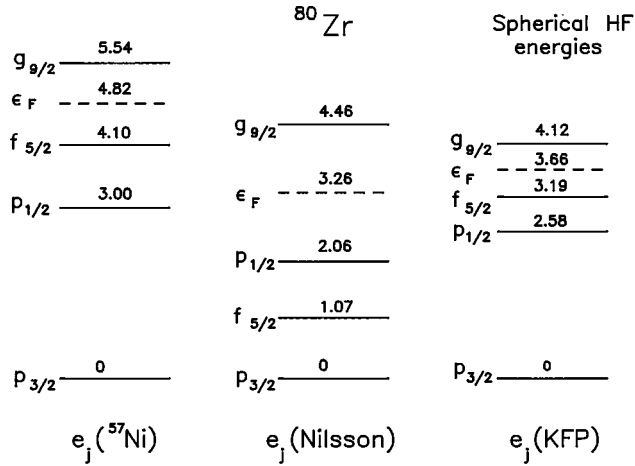
FIG. 2. Spherical Hartree-Fock single-particle energies ϵ_j for ^{80}Zr for three different choices of the energy e_j.

about the same relative spacings. The e_j(Nilsson) spectrum is also compressed relative to the $e_j(^{57}$Ni) spectrum, and it has the $f_{5/2}$ shell below the $p_{1/2}$ shell.

C. Deformation

The HF equation is solved for each choice of e_j. Triaxial shapes are considered as well as axially symmetric shapes. The first surprising result is the sheer multiplicity of solutions. For ^{76}Sr using $e_j(^{57}$Ni), there are eight distinct HF states: three are prolate ($\beta=0.091$, 0.194, 0.382), four are oblate ($\beta=-0.066$, -0.134, -0.329, -0.345), and the ground state is triaxial ($\beta=0.350$, $\gamma=169°$). For isotopes considered here, the typical number of HF states is 4–6. Axially symmetric HF states are often saddle points, which are relative minima in β and relative maxima in γ. To determine which states are saddle points, constraints were included for the quadrupole degrees of freedom

$$h' = h - \chi_{20}Q_{20} - \chi_{22}(Q_{22} + Q_{2-2}). \qquad (3.7)$$

For each HF state, the Lagrange multipliers χ_{20} and χ_{22} are varied to map out the energy surface in the neighborhood of the HF state, thereby determining whether the state is a saddle point. Of the eight ^{76}Sr states listed above, four are saddle points.

Figure 3 shows the deformation β for the lowest energy HF state (ground state). Figure 4 shows the prolate-oblate energy difference, which is the energy of the lowest prolate state minus the energy of the lowest oblate state. If this energy difference is large (small), then the deformation is stiff (soft) in γ. For ^{76}Sr and ^{80}Zr the deformations are large. However, e_j(Nilsson) gives a smaller β than the other two e_j, which is probably caused by the larger gap at the Fermi surface shown in Fig. 2. For the heavier isotopes the deformation decreases with mass number. For the magic nucleus ^{100}Sn the model space is filled, and the shape is spherical. The different choices for e_j give different shapes. They also give very different prolate-oblate energy differences. This confirms the early finding that the ground state shapes of
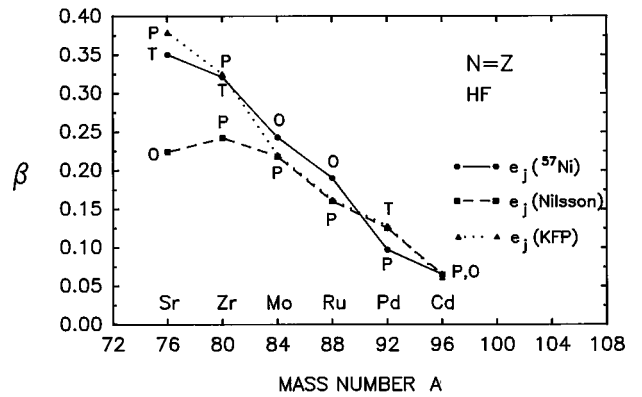

FIG. 3. Hartree-Fock quadrupole deformation β. The shapes are prolate (P), oblate (O), or triaxial (T).

these isotopes are very sensitive to the choice of parameters in the Hamiltonian [67,72,74]. For ^{76}Sr, the shape is triaxial for $e_j(^{57}$Ni), γ-soft oblate for e_j(Nilsson), and strongly deformed prolate for e_j(KFP). For ^{80}Zr, the shape is triaxial for $e_j(^{57}$Ni), and γ-soft prolate for the other two e_j. For ^{84}Mo, the shape is oblate for $e_j(^{57}$Ni), and γ-soft prolate for the other two e_j.

During the past 20 years there have been numerous investigations into the shape of ^{80}Zr. Early calculations found a γ-soft oblate shape [63], or a shape which is almost spherical or γ-soft oblate [66,67]. Early and later calculations found a prolate shape [43,61,64,65], or a γ-soft prolate shape [68,69]. Experiment finds that the shape of ^{80}Zr is triaxial or γ-soft with $\beta\approx0.4$ [72]. Apparently experiments have not yet determined the sign of the quadrupole moment, which would signify whether the shape is prolate or oblate.

IV. ISOSPIN GENERALIZED BCS

Although the isospin generalized BCS theory does not provide complete self-consistency in pair and shape degrees of freedom, it still serves several useful functions. (1) This theory shows how to choose the quasiparticle transformations so that all possible nucleon-nucleon pair modes can be contained in one wave function. (2) The BCS wave functions
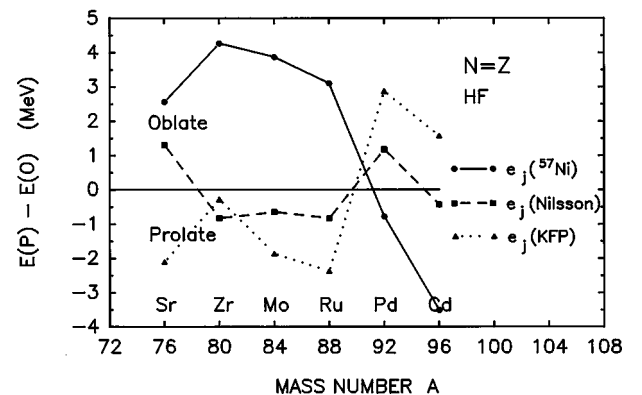

FIG. 4. Hartree-Fock prolate-oblate energy difference. This is the energy of the lowest prolate state minus the energy of the lowest oblate state.

will be used as trial input wave functions for HFB calculations. Because the BCS equations are much easier to solve than the HFB equation, this two step procedure is much more efficient than attempting to use HFB without having the BCS states as starting points. Because the pair gaps and quasiparticle coefficients are complex and the values of the phases are critical, it would be difficult to begin with HFB without having BCS as input.

A. Theory

The conventional BCS theory, which omits proton-neutron pairing, defines the quasiparticle operators $a^\dagger$ by a two-dimensional transformation of the particle operators $C^\dagger$

$$\begin{pmatrix} a^\dagger_\alpha \\ a_{\bar\alpha} \end{pmatrix} = \begin{pmatrix} u_\alpha & -v_\alpha \\ v_\alpha & u_\alpha \end{pmatrix} \begin{pmatrix} C^\dagger_\alpha \\ C_{\bar\alpha} \end{pmatrix}, \quad (4.1)$$

where $|\alpha\rangle$ is a HF single-particle orbital. The isospin generalized BCS theory [23] replaces Eq. (4.1) with the eight-dimensional transformation

$$\begin{pmatrix} \mathbf{a}^\dagger(\alpha) \\ \mathbf{a}(\alpha) \end{pmatrix} = \begin{pmatrix} u(\alpha) & -v(\alpha) \\ -v^*(\alpha) & u^*(\alpha) \end{pmatrix} \begin{pmatrix} \mathbf{C}^\dagger(\alpha) \\ \mathbf{C}(\alpha) \end{pmatrix}, \quad (4.2)$$

where $\mathbf{a}^\dagger(\alpha)$ and $\mathbf{C}^\dagger(\alpha)$ are the four-component vectors

$$\mathbf{a}^\dagger(\alpha) = \begin{pmatrix} a^\dagger_{\alpha 1} \\ a^\dagger_{\alpha 2} \\ a^\dagger_{\bar\alpha 1} \\ a^\dagger_{\bar\alpha 2} \end{pmatrix}, \quad \mathbf{C}^\dagger(\alpha) = \begin{pmatrix} C^\dagger_{\alpha p} \\ C^\dagger_{\alpha n} \\ C^\dagger_{\bar\alpha p} \\ C^\dagger_{\bar\alpha n} \end{pmatrix}. \quad (4.3)$$

Observe that each quasiparticle contains both proton and neutron components. In the ground state of a nucleus with $N=Z=$ even, time-reversal symmetry and isospin symmetry each create a degeneracy factor of two. Then the four-dimensional matrices $u(\alpha)$ and $v(\alpha)$ acquire the simplified forms

$$u(\alpha) = u_\alpha I, \quad (4.4)$$

where I is the four-dimensional unit matrix and

$$v(\alpha) = \begin{pmatrix} 0 & v_{\alpha 1} & v_{\alpha 2} & v_{\alpha 3} \\ -v_{\alpha 1} & 0 & v^*_{\alpha 3} & -v_{\alpha 2} \\ -v_{\alpha 2} & -v^*_{\alpha 3} & 0 & v^*_{\alpha 1} \\ -v_{\alpha 3} & v_{\alpha 2} & -v^*_{\alpha 1} & 0 \end{pmatrix}, \quad (4.5)$$

where $u_\alpha, v_{\alpha 2}$ are real and $v_{\alpha 1}, v_{\alpha 3}$ are complex. The isospin generalized pairing wave-function for the ground state of even $N=Z$ nuclei has the form

$$|\Phi_0\rangle = \prod_{\alpha > 0} (u_\alpha + v^*_{\alpha 1} C^\dagger_{\alpha p} C^\dagger_{\alpha n} + v_{\alpha 2} C^\dagger_{\alpha p} C^\dagger_{\bar\alpha p} + v^*_{\alpha 3} C^\dagger_{\alpha p} C^\dagger_{\bar\alpha n})$$

$$\times (u_\alpha + v_{\alpha 1} C^\dagger_{\bar\alpha p} C^\dagger_{\bar\alpha n} - v_{\alpha 2} C^\dagger_{\alpha n} C^\dagger_{\bar\alpha n} + v_{\alpha 3} C^\dagger_{\alpha n} C^\dagger_{\bar\alpha p})|0\rangle. \quad (4.6)$$

This wave function is the vacuum for the quasiparticles defined in Eq. (4.2). It includes $p\bar p$, $n\bar n$, and $p\bar n$ Cooper pairs, where the two nucleons are in time-reversed orbitals, as well as pn Cooper pairs, where the two nucleons are in identical orbitals. All of these different types of Cooper pairs can coexist in the same wave-function. If $v_{\alpha 1}$ and $v_{\alpha 3}$ equal zero, then the proton-neutron pairs vanish, and the wave function reduces to the usual BCS form with only proton-proton and neutron-neutron pairing. For each α, there is a quartet of single-particle orbitals $|\alpha p\rangle$, $|\alpha n\rangle$, $|\bar\alpha p\rangle$, and $|\bar\alpha n\rangle$. Each one of these orbitals has an occupation probability

$$v^2_\alpha = |v_{\alpha 1}|^2 + |v_{\alpha 2}|^2 + |v_{\alpha 3}|^2, \quad (4.7)$$

where $u^2_\alpha + v^2_\alpha = 1$. The wave function (4.6) is used to construct the HF Hamiltonian h and the pair potential Δ. In the BCS approximation one neglects those elements of h and Δ which connect one quartet of orbitals to another quartet. Then the HF Hamiltonian is block diagonal in the four-dimensional matrices $h(\alpha)$, which have the same structure as $u(\alpha)$ in Eq. (4.4). That is, $h(\alpha)$ is diagonal and four-fold degenerate, where the diagonal elements equal the HF single-particle energy

$$\epsilon_\alpha = \langle \alpha | e_j | \alpha \rangle + \sum_{\beta \tau'} \langle \alpha \tau \beta \tau' | v_a | \alpha \tau \beta \tau' \rangle v^2_\beta, \quad (4.8)$$

where τ is p or n. Similarly, the pair potential Δ is block diagonal in the four-dimensional matrices $\Delta(\alpha)$, which have the same structure as $v(\alpha)$ in Eq. (4.5). The components of the pair potential are

$$\Delta_{\alpha p, \bar\alpha p} = \sum_{\beta > 0} \langle \alpha \bar\alpha T=1 | v_a | \beta \bar\beta T=1 \rangle u_\beta v_{\beta 2}, \quad (4.9)$$

$$\text{Re}\,\Delta_{\alpha n, \bar\alpha p} = \sum_{\beta > 0} \langle \alpha \bar\alpha T=1 | v_a | \beta \bar\beta T=1 \rangle u_\beta \,\text{Re}\,v_{\beta 3}, \quad (4.10)$$

$$\text{Im}\,\Delta_{\alpha n, \bar\alpha p} = \sum_{\beta > 0} \langle \alpha \bar\alpha T=0 | v_a | \beta \bar\beta T=0 \rangle u_\beta \,\text{Im}\,v_{\beta 3}, \quad (4.11)$$

$$\text{Re}\,\Delta_{\alpha p, \alpha n} = \frac{1}{2} \sum_{\beta > 0} [\langle \alpha \alpha T=0 | v_a | \beta \beta T=0 \rangle$$
$$+ \langle \alpha \alpha T=0 | v_a | \bar\beta \bar\beta T=0 \rangle] u_\beta \,\text{Re}\,v_{\beta 1}, \quad (4.12)$$

$$\text{Im}\,\Delta_{\alpha p, \alpha n} = \frac{1}{2} \sum_{\beta > 0} [-\langle \alpha \alpha T=0 | v_a | \beta \beta T=0 \rangle$$
$$+ \langle \alpha \alpha T=0 | v_a | \bar\beta \bar\beta T=0 \rangle] u_\beta \,\text{Im}\,v_{\beta 1}. \quad (4.13)$$

The real part of $\Delta_{\alpha n, \bar\alpha p}$ contains $T=1$ Cooper pairs, which have occupation probabilities $|\text{Re}\,v_{\alpha 3}|^2$. The imaginary part of $\Delta_{\alpha n, \bar\alpha p}$ contains $T=0$ pairs, which have occupation prob-

abilities $|\mathrm{Im}\, v_{\alpha 3}|^2$. However $\Delta_{\alpha p, \alpha n}$ contains only $T = 0$ pairs. Also $\Delta_{\alpha p, \bar{\alpha} p}$ is real. From the four-dimensional matrices $h(\alpha)$ and $\Delta(\alpha)$, one constructs the eight-dimensional BCS energy matrix. The quasiparticle energies are the eigenvalues of this energy matrix, which are fourfold degenerate, and have the form

$$E_\alpha = [(\epsilon_\alpha - \lambda)^2 + \Delta_\alpha^2]^{1/2}, \tag{4.14}$$

where λ is the Fermi energy, and the pair potential Δ_α is the coherent sum of the contributions from each pair mode

$$\Delta_\alpha^2 = |\Delta_{\alpha p, \bar{\alpha} p}|^2 + |\Delta_{\alpha p, \bar{\alpha} n}|^2 + |\Delta_{\alpha p, \alpha n}|^2. \tag{4.15}$$

The eigenvectors of the eight-dimensional energy matrix can be obtained analytically, with the result that

$$u_\alpha = \left[\frac{1}{2} [1 + (\epsilon_\alpha - \lambda)/E_\alpha] \right]^{1/2}, \tag{4.16}$$

$$v_\alpha = \left[\frac{1}{2} [1 - (\epsilon_\alpha - \lambda)/E_\alpha] \right]^{1/2}, \tag{4.17}$$

$$v_{\alpha 1} = -v_\alpha (\Delta_{\alpha p, \alpha n}^* / \Delta_\alpha), \tag{4.18}$$

$$v_{\alpha 2} = -v_\alpha (\Delta_{\alpha p, \bar{\alpha} p} / \Delta_\alpha), \tag{4.19}$$

$$v_{\alpha 3} = -v_\alpha (\Delta_{\alpha p, \bar{\alpha} n}^* / \Delta_\alpha). \tag{4.20}$$

The Fermi energy λ is adjusted to constrain the particle number

$$N = Z = 2 \sum_{\alpha > 0} v_\alpha^2. \tag{4.21}$$

The coupled Eqs. (4.7)–(4.21) are solved by iteration to obtain the self-consistent values of u_α and $v_{\alpha i}$. Begin with the initial trial choices of u_α and $v_{\alpha i}$, and use Eqs. (4.8)–(4.15) to calculate the pair gaps and single-particle energies. Then use Eqs. (4.16)–(4.20) to calculate new values for u_α and $v_{\alpha i}$. Repeat this procedure until convergence is obtained. The value of Δ_α is different for each orbital $|\alpha\rangle$. So it is convenient to define average pair gaps $\bar{\Delta}$ for each of the different pair modes

$$\bar{\Delta}_{p\bar{p}} = -\bar{\Delta}_{n\bar{n}} = \frac{1}{m} \sum_{\alpha=1}^{m} |\Delta_{\alpha p, \bar{\alpha} p}|, \tag{4.22}$$

$$\bar{\Delta}_{p\bar{n}} = \frac{1}{m} \sum_{\alpha=1}^{m} |\Delta_{\alpha p, \bar{\alpha} n}|, \tag{4.23}$$

$$\bar{\Delta}_{pn} = \frac{1}{m} \sum_{\alpha=1}^{m} |\Delta_{\alpha p, \alpha n}|, \tag{4.24}$$

where $\bar{p}$ or $\bar{n}$ means that the nucleon occupies one of the time-reversed orbitals $|\bar{\alpha}\rangle$. The energy of the nucleus $E_{\mathrm{BCS}} = \langle H \rangle$ is evaluated using the BCS wave function (4.6).
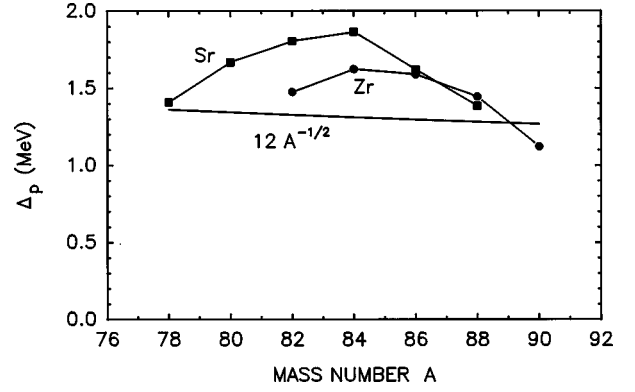

FIG. 5. Experimental proton pair gap Δ_p determined by odd-even mass difference P_p. Equation (4.25) is also shown.

B. Pair correlations

The isospin generalized BCS equations are solved for the $N = Z$ even isotopes with $A = 76$–96. The nucleon orbitals $|\alpha\rangle$ are taken from the HF calculations, and every HF state is used as the starting point for a BCS calculation. The pair potential Δ is calculated with the effective interaction determined from the Paris potential. The pair potential includes the multipole channels $J = 0,1,2,3,4,5,6,7,8,9$ and the isospin channels $T = 0,1$. If $e_j(^{57}\mathrm{Ni})$ is used, then the lowest energy state for $^{76}\mathrm{Sr}$ and $^{80}\mathrm{Zr}$ has $\Delta \approx 0.6\,\mathrm{MeV}$, and the pairing is entirely in the $T = 1$ channel. How does this compare to experimental values of Δ, which are given by odd-even mass differences? The experimental Δ has been parametrized as [77]

$$\Delta_{\mathrm{exp}} \approx \frac{12\,\mathrm{MeV}}{A^{1/2}}. \tag{4.25}$$

For $A = 80$, this gives $\Delta_{\mathrm{exp}} \approx 1.3\,\mathrm{MeV}$. The odd-even mass differences are

$$P_p = \frac{1}{4} [2 S_p(N,Z) - S_p(N,Z+1) - S_p(N,Z-1)], \tag{4.26}$$

$$P_n = \frac{1}{4} [2 S_n(N,Z) - S_n(N+1,Z) - S_n(N-1,Z)], \tag{4.27}$$

where the nucleon separation energies S are obtained from Ref. [78]. Figures 5 and 6 show the experimental values of Δ given by P_p and P_n. The lightest Sr and Zr isotopes have Δ in the vicinity of 1.3 MeV. Consequently the calculated values of Δ are significantly smaller than the experimental values. As has often been observed in the past, it is not easy to calculate pairing matrix elements from the bare nucleon-nucleon interaction with no free parameters, and it is difficult to use the same effective interaction to obtain good HF properties and good pairing properties. Most nuclear structure calculations use different effective interactions for the HF and pair potentials. To obtain better agreement between calculated and experimental pair gaps, a pairing scale parameter S_p is introduced. Every matrix element of the effective inter-
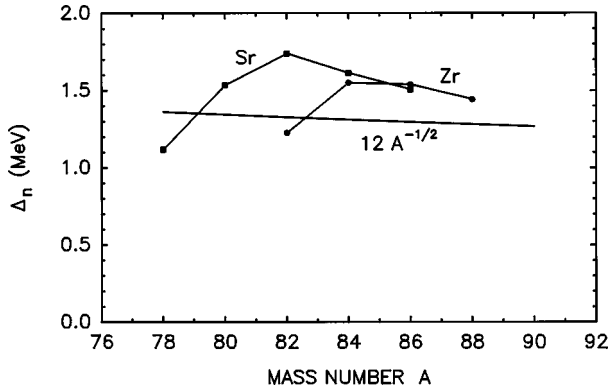
FIG. 6. Experimental neutron pair gap Δ_n determined by odd-even mass difference P_n. Equation (4.25) is also shown.

action which is used in the evaluation of Δ is multiplied by S_p. Matrix elements of the effective interaction which are used in the HF potential are left in their original form. Figure 7 shows how Δ varies with the parameter S_p for the lowest energy BCS state of ^{80}Zr. In this state there is only $T=1$ pairing. To obtain $\Delta \approx 1.3$ MeV, the value $S_p=1.45$ is adopted. Although $e_j(^{57}$Ni$)$ and $e_j($Nilsson$)$ give very different values of Δ at $S_p=1$ (no scaling), fortuitously they give very similar values of Δ at $S_p=1.45$. All BCS calculations are repeated using $S_p=1.45$.

We first consider the lowest energy BCS state for each isotope. The average pair gap $\bar{\Delta}$ is shown in Fig. 8. If $e_j(^{57}$Ni$)$ is used, then ^{76}Sr, ^{80}Zr, and ^{84}Mo have $T=1$ pair correlations, whereas ^{88}Ru and ^{92}Pd have coexistence of the $T=0$ pair superfluid and the $T=1$ pair superfluid, and ^{96}Cd has $T=0$ pair correlations. If $e_j($Nilsson$)$ is used, then ^{76}Sr has $T=1$ pairing, ^{92}Pd has $T=0$ pairing, while ^{80}Zr and ^{96}Cd have coexistence of the $T=0$ pair phase and the $T=1$ pair phase. If $e_j($KFP$)$ is used, then ^{76}Sr, ^{80}Zr, and ^{96}Cd have $T=1$ pairing, ^{92}Pd has $T=0$ pairing, and ^{84}Mo has coexisting phases with $T=0$ pairing and $T=1$ pairing. The claim has been made that $T=0$ pairing and $T=1$ pairing never coexist in the isospin generalized BCS theory. This calculation clearly demonstrates that for a given Hamiltonian H, some isotopes have the $T=0$ pairing superfluid and the $T=1$ pairing superfluid coexisting in the same BCS ground state wave function.
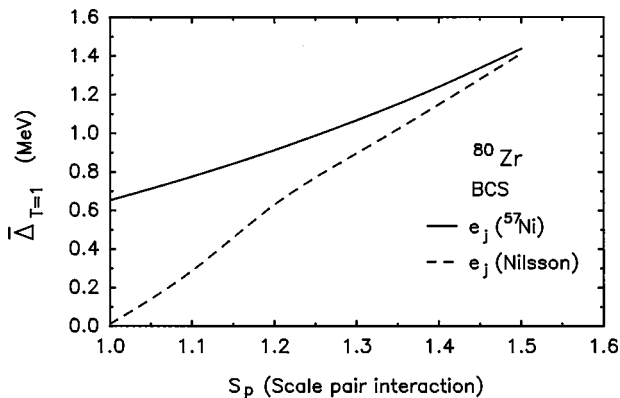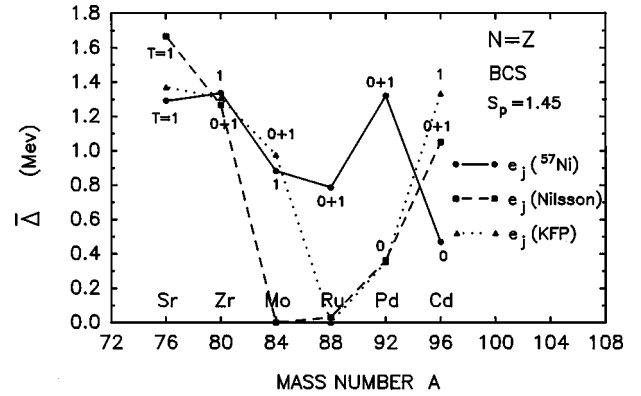

FIG. 8. Average pair gap $\bar{\Delta}$ versus mass number A for isospin generalized BCS calculations.

In order to compare the energy provided by the different types of Cooper pairs, the BCS equations are solved in several different ways for every HF state. (1) In the initial trial wave function choose all components of $v_{\alpha i} \neq 0$. Then the final self-consistent wave function will contain the types of Cooper pairs which minimize the energy. (2) Choose initial values $v_{\alpha 2} \neq 0$ and the other $v_{\alpha i}=0$. Then the final wave function will contain only $p\bar{p}$ and $n\bar{n}$ pairs. [This state is degenerate with the state containing only $p\bar{n}$ ($T=1$) pairs.] (3) Choose initial values Im $v_{\alpha 3} \neq 0$ and the other components of $v_{\alpha i}=0$. Then the final wave function will contain only $p\bar{n}$ ($T=0$) pairs. (4) Choose initial values $v_{\alpha 1} \neq 0$ and the other $v_{\alpha i}=0$. Then the final wave function will contain only pn ($T=0$) pairs. All of these different solutions of the BCS equations are self-consistent.

Figures 9–11 compare the energies obtained with these four BCS states. All four BCS states are based upon the same HF state, which is the one that leads to the BCS state of lowest energy. For ^{76}Sr and ^{80}Zr $T=1$ pairing gives significantly more binding energy than $T=0$ pairing. In several instances the ground state with $T=0$ pairing and $T=1$ pairing is slightly below the state with only $T=1$ pairing; these include ^{80}Zr using $e_j($Nilsson$)$, ^{84}Mo using $e_j($KFP$)$, and ^{88}Ru using $e_j(^{57}$Ni$)$. In ^{92}Pd $T=0$ pairing provides substantially more binding energy than $T=1$ pairing if $e_j($Nilsson$)$

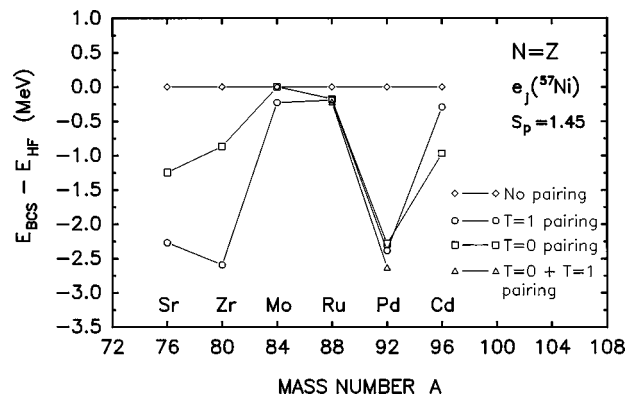FIG. 7. BCS average pair gap $\bar{\Delta}$ versus the scale parameter S_p.

FIG. 9. Difference between BCS energy and Hartree-Fock energy for each type of Cooper pair. The $e_j(^{57}$Ni$)$ single nucleon energies are used.
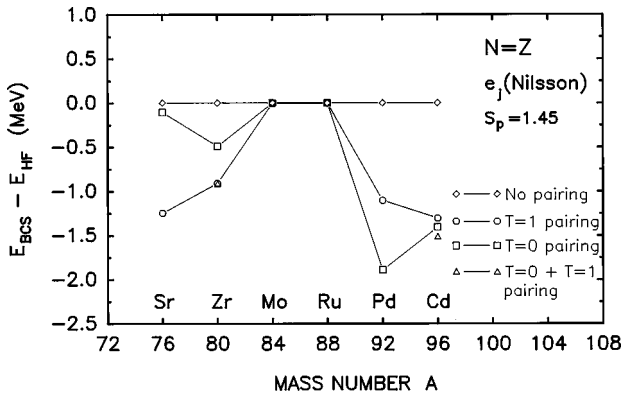
FIG. 10. Difference between BCS energy and Hartree-Fock energy for each type of Cooper pair. The e_j(Nilsson) single nucleon energies are used.

FIG. 12. BCS quadrupole deformation β. The shapes are prolate (P), oblate (O), or triaxial (T).

or e_j(KFP) are used; however, for $e_j(^{57}$Ni) the ground state with $T=0$ pairing and $T=1$ pairing is 0.247 MeV below the state with only $T=1$ pairing. For ^{96}Cd using e_j(Nilsson), the ground state with $T=0$ pairing and $T=1$ pairing is 0.106 MeV below the state with only $T=0$ pairing.

If two mean field states are close in energy, then the residual interaction will sometimes connect them, thereby producing a mixed state which incorporates properties of both of the original states. A typical example is two HF states with different deformation, as prolate and oblate. Another example might be two BCS states, where one has $T=0$ pairing and the other has $T=1$ pairing. Mixing these two BCS states would yield a state with both $T=0$ and $T=1$ pairing. In the previous paragraph there are examples of a BCS ground state with both $T=0$ and $T=1$ pairing which is close in energy to another BCS state with only $T=0$ or $T=1$ pairing. Since the ground state already includes both types of pairing, it would be redundant to mix this ground state with another state which has only one type of pairing. (Both BCS states use the same set of HF single nucleon orbitals and the same HF deformation.) If the upper state has only $T=0$ (or $T=1$) pairing, then including a small amount of $T=1$ (or $T=0$) pairing in the upper state and resuming iterations to obtain self-consistency would cause it to become identical to the
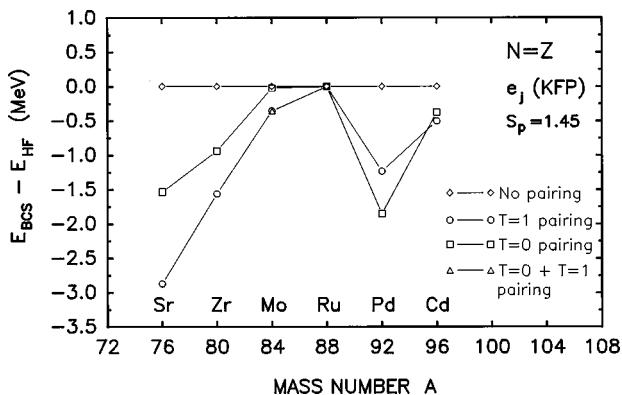
ground state. Conversely, if one begins with the ground state and then turns off the $T=1$ (or $T=0$) pair interaction, then iterations toward self-consistency will end with the ground state reverting to the upper state with only $T=0$ (or $T=1$) pairing.

C. Deformation

Figure 12 shows the deformation for the lowest energy BCS state. Figure 13 shows the BCS prolate-oblate energy difference. These can be compared to the corresponding HF Figs. 3 and 4. Whereas HF has some triaxial ground states, the BCS ground states are all axially symmetric. For ^{80}Zr the shape is γ-soft prolate for e_j(Nilsson) and e_j(KFP), and oblate for $e_j(^{57}$Ni).

V. HARTREE-FOCK-BOGOLIUBOV

To obtain complete self-consistency in both Hartree-Fock and BCS degrees of freedom, it is necessary to perform HFB calculations.

A. Theory

In the past I have done HFB calculations for $p\bar{p}, n\bar{n}$, and $p\bar{n}$ Cooper pairs, and separately for pn Cooper pairs. How-

FIG. 11. Difference between BCS energy and Hartree-Fock energy for each type of Cooper pair. The e_j(KFP) single nucleon energies are used.
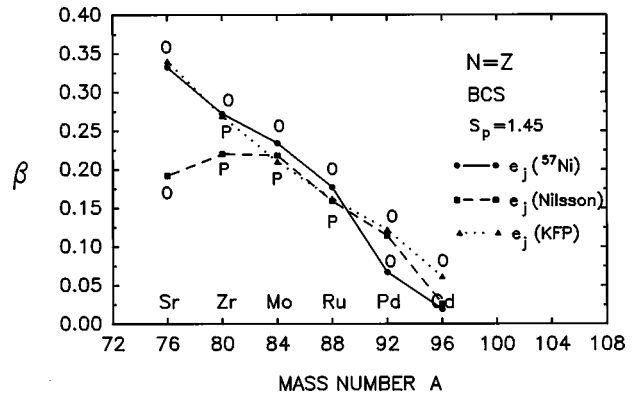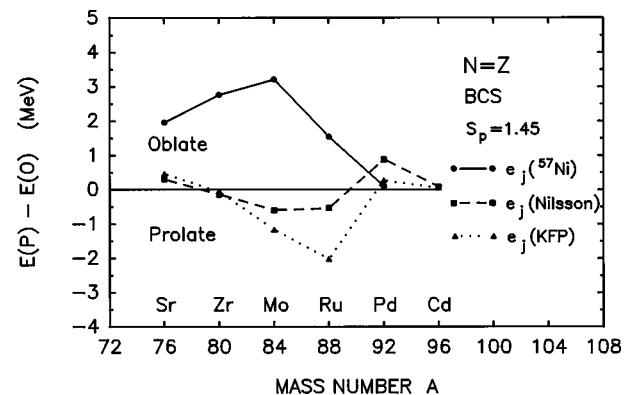

FIG. 13. BCS prolate-oblate energy difference. This is the energy of the lowest prolate state minus the energy of the lowest oblate state.

ever this is the first time I am performing HFB calculations which simultaneously include $p\bar{p}, n\bar{n}, p\bar{n}$ and pn Cooper pairs. Consequently the isospin structure of the theory will be presented in some detail. Parity is a conserved symmetry. For each parity, the quasiparticle operators $a^\dagger$ are defined by a unitary transformation of the particle operators $C^\dagger$

$$\begin{pmatrix} \mathbf{a}^\dagger \\ \mathbf{a} \end{pmatrix} = \begin{pmatrix} U & V \\ V^* & U^* \end{pmatrix} \begin{pmatrix} \mathbf{C}^\dagger \\ \mathbf{C} \end{pmatrix}, \tag{5.1}$$

where the vectors $\mathbf{a}^\dagger$ and $\mathbf{C}^\dagger$ are

$$\mathbf{a}^\dagger = \begin{pmatrix} \mathbf{a}_1^\dagger \\ \mathbf{a}_2^\dagger \\ \mathbf{a}_{\bar{1}}^\dagger \\ \mathbf{a}_{\bar{2}}^\dagger \end{pmatrix}, \quad \mathbf{C}^\dagger = \begin{pmatrix} \mathbf{C}_p^\dagger \\ \mathbf{C}_n^\dagger \\ \mathbf{C}_{\bar{p}}^\dagger \\ \mathbf{C}_{\bar{n}}^\dagger \end{pmatrix}. \tag{5.2}$$

The vector $\mathbf{C}_p^\dagger$ has dimension M and contains the components $C_{ip}^\dagger$, where M is the number of single proton states $|i\rangle = |nljm\rangle$ with $m-1/2$ equal to an even integer, and similarly for the vector $\mathbf{C}_n^\dagger$. The vector $\mathbf{C}_{\bar{p}}^\dagger$ has dimension M and contains the components $C_{\bar{i}p}^\dagger$ where $|\bar{i}\rangle$ is the time reverse of $|i\rangle$, i.e., $(-1)^{j-m+l}|nlj-m\rangle$, and similarly for the vector $\mathbf{C}_{\bar{n}}^\dagger$. The vector $\mathbf{a}_1^\dagger$ has dimension M with components $a_{j1}^\dagger$, where $j=1,2\cdots M$, and similarly for $\mathbf{a}_2^\dagger$, $\mathbf{a}_{\bar{1}}^\dagger$, and $\mathbf{a}_{\bar{2}}^\dagger$. For the ground state of a nucleus with $N=Z=$ even, time-reversal symmetry and isospin symmetry each create a degeneracy factor of two in the quasiparticle energies. Then the matrices U and V have the forms

$$U = \begin{pmatrix} U_1 & 0 & 0 & 0 \\ 0 & U_1 & 0 & 0 \\ 0 & 0 & U_1 & 0 \\ 0 & 0 & 0 & U_1 \end{pmatrix}, \tag{5.3}$$

$$V = - \begin{pmatrix} 0 & V_1 & V_2 & V_3 \\ -V_1 & 0 & V_3^* & -V_2 \\ -V_2 & -V_3^* & 0 & V_1^* \\ -V_3 & V_2 & -V_1^* & 0 \end{pmatrix}, \tag{5.4}$$

where the matrices U_1, V_1, V_2, and V_3 have dimension $M \times M$. Also U_1 and V_2 are real, whereas V_1 and V_3 are complex. Combining Eqs. (5.1)–(5.4), the quasiparticle operators are explicitly given as

$$a_{j1}^\dagger = \sum_i [(U_1)_{ji} C_{ip}^\dagger - (V_1)_{ji} C_{in} - (V_2)_{ji} C_{\bar{i}p} - (V_3)_{ji} C_{\bar{i}n}], \tag{5.5}$$

$$a_{j2}^\dagger = \sum_i [(U_1)_{ji} C_{in}^\dagger + (V_1)_{ji} C_{ip} - (V_3^*)_{ji} C_{\bar{i}p} + (V_2)_{ji} C_{\bar{i}n}], \tag{5.6}$$

$$a_{\bar{j}1}^\dagger = \sum_i [(U_1)_{ji} C_{\bar{i}p}^\dagger + (V_2)_{ji} C_{ip} + (V_3^*)_{ji} C_{in} - (V_1^*)_{ji} C_{\bar{i}n}], \tag{5.7}$$

$$a_{\bar{j}2}^\dagger = \sum_i [(U_1)_{ji} C_{\bar{i}n}^\dagger + (V_3)_{ji} C_{ip} - (V_2)_{ji} C_{in} + (V_1^*)_{ji} C_{\bar{i}p}]. \tag{5.8}$$

The HFB equation will be solved by an iterative procedure. On the first iteration, the HFB trial wave function is given by the isospin generalized BCS wave function (4.6), and the HFB quasiparticle transformation (5.1) is given by the BCS quasiparticle transformation (4.2). Therefore on the first iteration (but not on later iterations), the index j in Eqs. (5.5)–(5.8) is equivalent to the index α in Eq. (4.3). Then the HFB starting values are

$$(U_1)_{\alpha i} = u_\alpha D_{\alpha i}, \tag{5.9}$$

$$(V_1)_{\alpha i} = v_{\alpha 1} D_{\alpha i}, \tag{5.10}$$

$$(V_2)_{\alpha i} = v_{\alpha 2} D_{\alpha i}, \tag{5.11}$$

$$(V_3)_{\alpha i} = v_{\alpha 3} D_{\alpha i}, \tag{5.12}$$

where $D_{\alpha i}$ is given by the HF orbitals (3.4) and $v_{\alpha i}$ is given by the BCS state (4.6).

The density matrix and the pairing tensor

$$\rho_{ij} = \langle C_j^\dagger C_i \rangle, \tag{5.13}$$

$$t_{ij} = \langle C_j C_i \rangle, \tag{5.14}$$

are evaluated with respect to the HFB quasiparticle vacuum, so that

$$\rho = V^\dagger V, \tag{5.15}$$

$$t = V^\dagger U. \tag{5.16}$$

Substituting Eq. (5.4) into Eq. (5.15), and using the unitarity constraint

$$U^\dagger U + \tilde{V} V^* = I, \tag{5.17}$$

it follows that ρ is block diagonal

$$\rho = \begin{pmatrix} \rho_{pp} & 0 & 0 & 0 \\ 0 & \rho_{pp} & 0 & 0 \\ 0 & 0 & \rho_{pp} & 0 \\ 0 & 0 & 0 & \rho_{pp} \end{pmatrix}, \tag{5.18}$$

where

$$(\rho_{\tau_1 \tau_2})_{ij} = \rho_{i\tau_1, j\tau_2}, \tag{5.19}$$

and

$$\rho_{pp} = \rho_{nn} = \rho_{\bar{p}\bar{p}} = \rho_{\bar{n}\bar{n}}, \tag{5.20}$$

$$\rho_{pp} = V_1^\dagger V_1 + V_2^\dagger V_2 + V_3^\dagger V_3. \quad (5.21)$$

The $M \times M$ matrix ρ_{pp} is real and symmetric. The structure of the pairing tensor is found by substituting Eqs. (5.3) and (5.4) into Eq. (5.16), so that

$$t = \begin{pmatrix} 0 & t_{pn} & t_{p\bar{p}} & t_{p\bar{n}} \\ -t_{pn} & 0 & t_{p\bar{n}}^* & -t_{p\bar{p}} \\ -t_{p\bar{p}} & -t_{p\bar{n}}^* & 0 & t_{pn}^* \\ -t_{p\bar{n}} & t_{p\bar{p}} & -t_{pn}^* & 0 \end{pmatrix}, \quad (5.22)$$

where

$$(t_{\tau_1 \tau_2})_{ij} = t_{i\tau_1, j\tau_2}, \quad (t_{\tau_1 \bar{\tau}_2})_{ij} = t_{i\tau_1, \bar{j}\tau_2}, \quad (5.23)$$

and

$$t_{p\bar{p}} = -t_{n\bar{n}}, \quad (5.24)$$

$$t_{pn} = V_1^\dagger U_1, \quad (5.25)$$

$$t_{p\bar{p}} = V_2^\dagger U_1, \quad (5.26)$$

$$t_{p\bar{n}} = V_3^\dagger U_1. \quad (5.27)$$

The $M \times M$ matrices t_{pn}, $t_{p\bar{p}}$, and $t_{p\bar{n}}$ are symmetric. Also, t_{pn} and $t_{p\bar{n}}$ are complex, whereas $t_{p\bar{p}}$ is real.

The HF Hamiltonian and HF potential are

$$h = e + \mathcal{U}, \quad (5.28)$$

$$\mathcal{U}_{ij} = \sum_{kl} \langle ik | v_a | jl \rangle \rho_{lk}. \quad (5.29)$$

Since ρ is real with the form given in Eq. (5.18), and since the nucleon-nucleon interaction is time-reversal invariant and conserves isospin projection, it follows that the HF Hamiltonian has the structure

$$h = \begin{pmatrix} h_{pp} & 0 & 0 & 0 \\ 0 & h_{pp} & 0 & 0 \\ 0 & 0 & h_{pp} & 0 \\ 0 & 0 & 0 & h_{pp} \end{pmatrix}, \quad (5.30)$$

where

$$(h_{pp})_{ij} = \langle i | e | j \rangle + \sum_{kl>0,\tau} [\langle ip, k\tau | v_a | jp, l\tau \rangle$$

$$+ \langle ip, \bar{k}\tau | v_a | jp, \bar{l}\tau \rangle](\rho_{pp})_{lk}, \quad (5.31)$$

and the $M \times M$ matrix h_{pp} is real and symmetric.

The pair potential is

$$\Delta_{ij} = \frac{1}{2} \sum_{kl} \langle ij | v_a | kl \rangle t_{kl}. \quad (5.32)$$

From the symmetries of the nucleon-nucleon interaction and the form of the pairing tensor given in Eq. (5.22), it follows that the pair potential has the structure

$$\Delta = \begin{pmatrix} 0 & \Delta_{pn} & \Delta_{p\bar{p}} & \Delta_{p\bar{n}} \\ -\Delta_{pn} & 0 & \Delta_{p\bar{n}}^* & -\Delta_{p\bar{p}} \\ -\Delta_{p\bar{p}} & -\Delta_{p\bar{n}}^* & 0 & \Delta_{pn}^* \\ -\Delta_{p\bar{n}} & \Delta_{p\bar{p}} & -\Delta_{pn}^* & 0 \end{pmatrix}, \quad (5.33)$$

where

$$\Delta_{p\bar{p}} = -\Delta_{n\bar{n}}, \quad (5.34)$$

and the subscript notation is the same as in Eq. (5.23). The components of the pair potential are

$$(\Delta_{p\bar{p}})_{ij} = \sum_{kl>0} \langle i\bar{j}T=1 | v_a | k\bar{l}T=1 \rangle (t_{p\bar{p}})_{kl}, \quad (5.35)$$

$$\mathrm{Re}(\Delta_{p\bar{n}})_{ij} = \sum_{kl>0} \langle i\bar{j}T=1 | v_a | k\bar{l}T=1 \rangle \mathrm{Re}(t_{p\bar{n}})_{kl}, \quad (5.36)$$

$$\mathrm{Im}(\Delta_{p\bar{n}})_{ij} = \sum_{kl>0} \langle i\bar{j}T=0 | v_a | k\bar{l}T=0 \rangle \mathrm{Im}(t_{p\bar{n}})_{kl}, \quad (5.37)$$

$$\mathrm{Re}(\Delta_{pn})_{ij} = \frac{1}{2} \sum_{kl>0} [\langle ijT=0 | v_a | klT=0 \rangle$$

$$+ \langle ijT=0 | v_a | \bar{k}\bar{l}T=0 \rangle] \mathrm{Re}(t_{pn})_{kl}, \quad (5.38)$$

$$\mathrm{Im}(\Delta_{pn})_{ij} = \frac{1}{2} \sum_{kl>0} [\langle ijT=0 | v_a | klT=0 \rangle$$

$$- \langle ijT=0 | v_a | \bar{k}\bar{l}T=0 \rangle] \mathrm{Im}(t_{pn})_{kl}. \quad (5.39)$$

The $M \times M$ matrices Δ_{pn}, $\Delta_{p\bar{p}}$, and $\Delta_{p\bar{n}}$ are symmetric. Also, Δ_{pn} and $\Delta_{p\bar{n}}$ are complex, whereas $\Delta_{p\bar{p}}$ is real. The real part of $\Delta_{p\bar{n}}$ contains $T=1$ pairs and the imaginary part of $\Delta_{p\bar{n}}$ contains $T=0$ pairs. However Δ_{pn} contains only $T=0$ pairs.

The HFB energy is

$$E_{\mathrm{HFB}} = \langle H \rangle = \mathrm{Tr}\left[\left(e + \frac{1}{2}\mathcal{U}\right)\rho + \frac{1}{2}\Delta t^\dagger\right]. \quad (5.40)$$

The HFB equation is

$$\begin{pmatrix} (h-\lambda) & \Delta \\ -\Delta^* & -(h-\lambda)^* \end{pmatrix} \begin{pmatrix} U_j \\ V_j \end{pmatrix} = E_j \begin{pmatrix} U_j \\ V_j \end{pmatrix}. \quad (5.41)$$

There is a fourfold degeneracy in the quasiparticle energies E_j. The complex HFB energy matrix has dimension $8M \times 8M$. It include all pair modes discussed in this article.
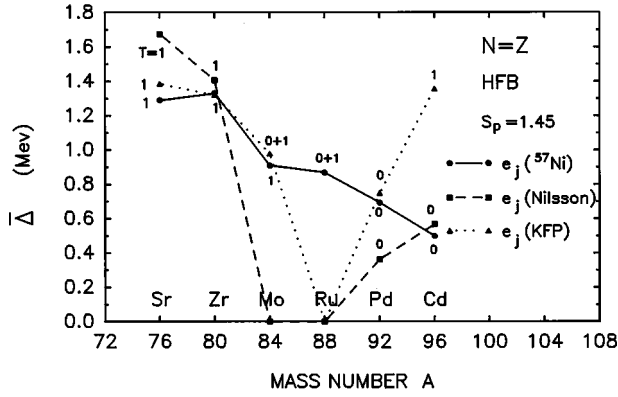
FIG. 14. Average pair gap $\bar{\Delta}$ versus mass number A for HFB calculations.

FIG. 15. Difference between HFB energy and Hartree-Fock energy for each pair mode. The $e_j(^{57}\text{Ni})$ single nucleon energies are used.

There are limiting cases: If $p\bar{p}$, $n\bar{n}$, and $p\bar{n}$ pairs are included, but pn pairs are omitted, then the energy matrix becomes block diagonal, and separates into two $4M \times 4M$ matrices. This is achieved by choosing $V_1 = 0$ in the trial wave function, then $V_1 = 0$ in the final self-consistent wave function. If $p\bar{p}$ and $n\bar{n}$ pairs are included, but $p\bar{n}$ and pn pairs are omitted, then the energy matrix separates into four $2M \times 2M$ matrices. This is achieved by choosing $V_1 = V_3 = 0$ in the trial wave function. If pn pairs are included, but all others are omitted, then the energy matrix separates into four $2M \times 2M$ matrices. This is achieved by choosing $V_2 = V_3 = 0$ in the trial wave function. If $p\bar{n}$ ($T=0$) pairs are included, but all others are omitted, then the energy matrix separates into four $2M \times 2M$ matrices. This is achieved by choosing $V_1 = V_2 = \text{Re } V_3 = 0$ and $\text{Im } V_3 \neq 0$ in the trial wave function. All of these provide self-consistent wave functions. The HFB equation is solved by iteration. On each iteration, the symmetries in ρ, t, h, and Δ [Eqs. (5.18), (5.22), (5.30), and (5.33)] are preserved. These are examples of propagating symmetries.

It has been demonstrated [23] that the HFB ground state wave function for even $N=Z$ nuclei can be given in the simple form of Eq. (4.6). This is provided by the quasicanonical basis: The HFB density matrix ρ is fourfold degenerate. The quartet of eigenvectors $|\alpha p\rangle$, $|\alpha n\rangle$, $|\bar{\alpha} p\rangle$, and $|\bar{\alpha} n\rangle$ correspond to the same eigenvalue v_α^2. This basis also provides a convenient way to characterize the HFB pair potential Δ. Average pair gaps $\bar{\Delta}$ can be defined for each of the different pair modes by representing Δ in the quasicanonical basis, and then using Eqs. (4.22)–(4.24).

B. Pair correlations

In Sec. IV B every HF state was used to obtain four different BCS wave functions, corresponding to different combinations of pair modes. Now every one of these BCS states is used as the initial trial wave function for a HFB calculation. The final result is a multiplicity of self-consistent HFB wave functions, which have different deformations and different types of Cooper pairs.

Now we consider the lowest energy HFB state for each isotope. The average pair gap $\bar{\Delta}$ is shown in Fig. 14. If
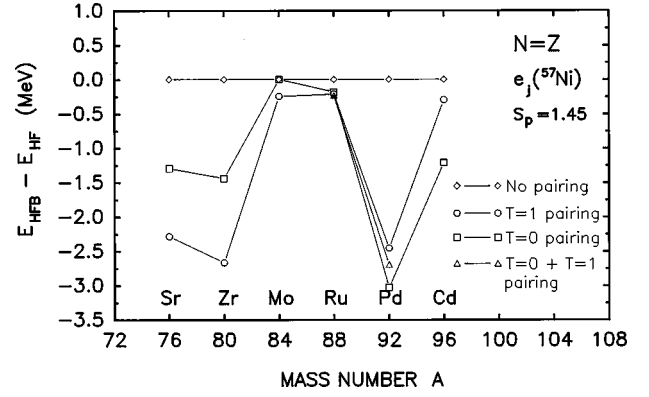
$e_j(^{57}\text{Ni})$ is used, then ^{76}Sr, ^{80}Zr, and ^{84}Mo have $T=1$ pair correlations, while ^{88}Ru has coexistence of the $T=0$ ($p\bar{n}$) pair superfluid and the $T=1$ pair superfluid, and ^{92}Pd and ^{96}Cd have $T=0$ (pn) pair correlations. If $e_j(\text{Nilsson})$ is used, then ^{76}Sr and ^{80}Zr have $T=1$ pairing, ^{84}Mo and ^{88}Ru have no pairing, and ^{92}Pd and ^{96}Cd have $T=0$ (pn) pairing. If $e_j(\text{KFP})$ is used, then ^{76}Sr, ^{80}Zr, and ^{96}Cd have $T=1$ pairs, ^{84}Mo has coexistence of the $T=0$ (pn) pair phase and the $T=1$ pair phase, ^{88}Ru has no pairing, and ^{92}Pd has two degenerate states with different deformations: one with $T=0$ (pn) pairs and one with $T=0$ ($p\bar{n}$) pairs. This calculation demonstrates that for a given Hamiltonian H, some isotopes have a $T=0$ pair superfluid and a $T=1$ pair superfluid coexisting in the same HFB ground state wave function.

The HFB energies can be compared for each of the different types of Cooper pairs. This is accomplished by comparing the lowest energy HFB state to other HFB states which originate from the same HF state. These different HFB states have different pair modes. The relative energies of these various HFB states are shown in Figs. 15–17. Figure 15 shows the relative HFB energies for $e_j(^{57}\text{Ni})$. For ^{76}Sr and ^{80}Zr, $T=1$ pairing provides significantly more binding energy than $T=0$ pairing. In ^{88}Ru the mixed phases ground state with $T=0$ and $T=1$ pairing is slightly below the state
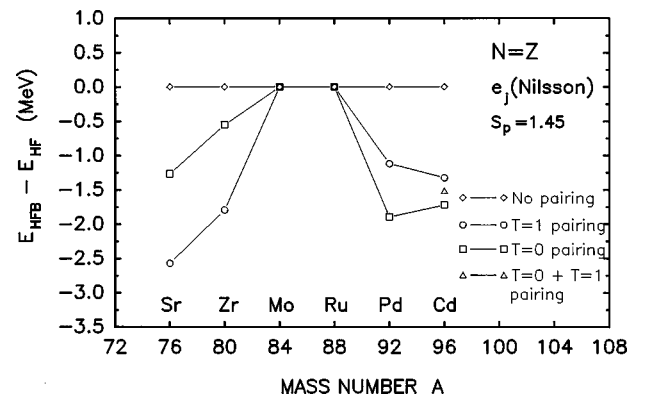

FIG. 16. Difference between HFB energy and Hartree-Fock energy for each pair mode. The $e_j(\text{Nilsson})$ single nucleon energies are used.
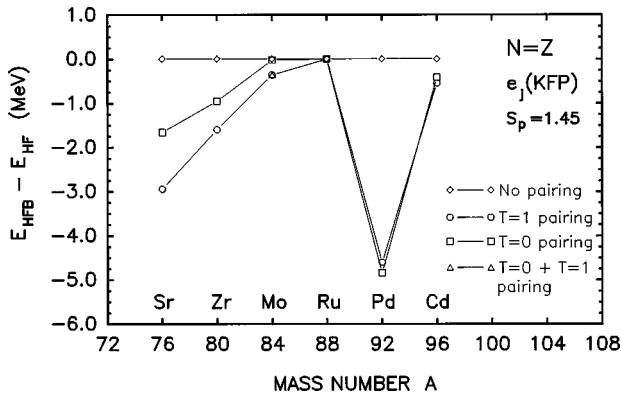
FIG. 17. Difference between HFB energy and Hartree-Fock energy for each pair mode. The e_j(KFP) single nucleon energies are used.

FIG. 19. HFB prolate-oblate energy difference. This is the energy of the lowest prolate state minus the energy of the lowest oblate state.

with only $T=1$ pairing. For ^{92}Pd the lowest energy state has $T=0$ (pn) Cooper pairs, while there is a higher energy state with the mixed phases containing $T=0$ ($p\bar{n}$) Cooper pairs and $T=1$ Cooper pairs. For ^{96}Cd $T=0$ pairing gives substantially more binding energy than $T=1$ pairing. Figure 16 shows the relative HFB energies for e_j(Nilsson). For ^{76}Sr and ^{80}Zr, $T=1$ pairing provides substantially more binding energy than $T=0$ pairing. For ^{92}Pd and ^{96}Cd, $T=0$ pairing provides significantly more binding than $T=1$ pairing. For ^{96}Cd the lowest energy state has $T=0$ (pn) Cooper pairs, while there is a higher energy state with the mixed phases containing $T=0$ ($p\bar{n}$) Cooper pairs and $T=1$ Cooper pairs. Figure 17 shows the relative HFB energies for e_j(KFP). For ^{76}Sr and ^{80}Zr, $T=1$ pairing provides significantly more binding energy than $T=0$ pairing. For ^{84}Mo the mixed phases ground state with $T=0$ and $T=1$ pairing is slightly below the state with only $T=1$ pairing. For ^{92}Pd the $T=0$ pairing state is 0.241 MeV below the $T=1$ pairing state. For ^{96}Cd the $T=1$ pairing state is only 0.131 MeV below the $T=0$ pairing state.

C. Deformation

Figure 18 shows the deformation for the lowest energy HFB state. Figure 19 shows the HFB prolate-oblate energy
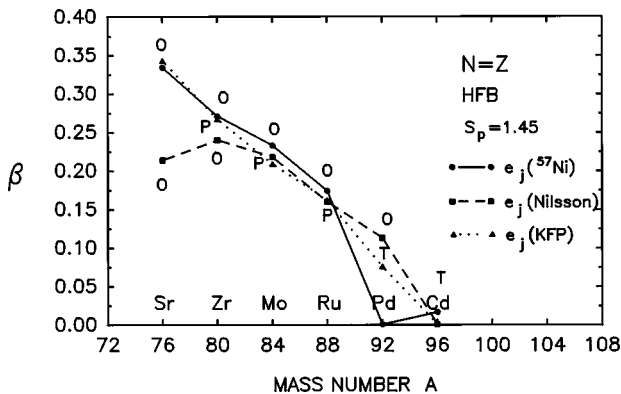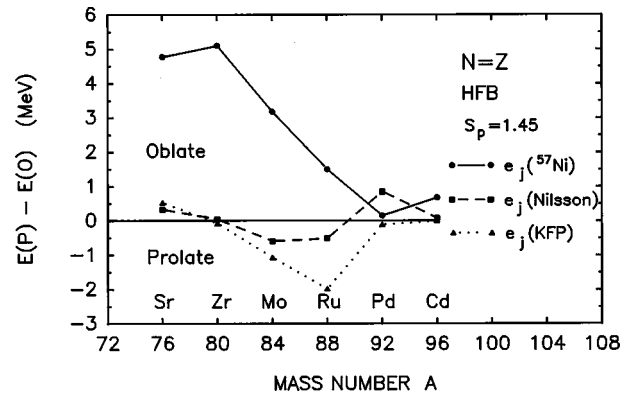

FIG. 18. HFB quadrupole deformation β. The shapes are prolate (P), oblate (O), or triaxial (T).

difference. These can be compared to the corresponding HF Figs. 3 and 4 and the BCS Figs. 12 and 13. HF, BCS, and HFB give comparable magnitudes for the quadrupole deformation β. However, whether the shape is prolate, oblate, or triaxial varies, as one goes from HF to BCS to HFB. Also, HF, BCS, and HFB give similar systematics for the prolate-oblate energy difference. However, if e_j(^{57}Ni) is used, then BCS gives smaller magnitudes for this energy difference than HF, and HFB restores the larger magnitudes. For ^{76}Sr, the shape is oblate for all three choices of e_j. However, for e_j(^{57}Ni) the oblate shape is strongly deformed; whereas for the other two choices of e_j the prolate shape is only 0.3–0.5 MeV above the oblate shape, so that the oblate shape is very γ soft. For ^{80}Zr, the shape is strongly deformed oblate for e_j(^{57}Ni); however for the other two choices of e_j the shape is very γ soft, with almost degenerate prolate and oblate shapes. For e_j(Nilsson) the oblate shape is only 0.039 MeV below the prolate shape, and for e_j(KFP) the prolate shape is just 0.082 MeV below the oblate shape. For ^{84}Mo, the shape is oblate for e_j(^{57}Ni), and γ-soft prolate for the other two e_j. For ^{88}Ru, the shape is γ-soft oblate for e_j(^{57}Ni), and γ-soft prolate for the other two e_j. For ^{92}Pd, the shape is almost spherical for e_j(^{57}Ni), γ-soft oblate for e_j(Nilsson), and γ-soft triaxial ($\gamma=-4.5°$) for e_j(KFP). For ^{96}Cd, the values of β are very small for all three choices of e_j.

These calculations show that different choices for the single-particle energies e_j give different ground state shapes and different prolate-oblate energy differences. This provides an opportunity for experiment to shed light upon appropriate choices for parameters in the Hamiltonian H. For example, if experiments find that ^{80}Zr does not have an oblate shape, then this would eliminate e_j(^{57}Ni) as an appropriate choice for HFB calculations in ^{80}Zr with this nucleon-nucleon interaction. The interpretation would be that the monopole components of the interaction are not finely tuned to provide the correct shifts in the energies of the j shells as the mass number changes from ^{57}Ni to ^{80}Zr. This would not be surprising, since the monopole components of the interaction were adjusted to give good spectra for the Ni isotopes, rather than the Zr isotopes. Correct values for the energies of the j shells in ^{80}Zr might then be obtained by using e_j(Nilsson) or e_j(KFP), rather than e_j(^{57}Ni).

VI. FLUCTUATIONS

Mean field theories include collective modes by violating symmetries of the nucleon-nucleon Hamiltonian H. For example, although H is rotationally invariant, mean field theories describe deformation by using fields and wave functions which are not rotationally invariant. The angular momentum J is not a good quantum number for these wave functions. This approach is adopted in Hartree-Fock and Nilsson calculations.

A. Number fluctuations

In a similar manner the BCS and HFB mean field theories describe pair correlations by using wave functions which do not conserve the particle number. These wave functions have the correct average proton and neutron numbers [Eq. (4.21)], but there are fluctuations in the proton and neutron numbers ΔZ and ΔN. For an even $Z=N$ nucleus, $\Delta Z=\Delta N$. The fluctuation in the neutron number is given by

$$(\Delta N)^2=\langle \hat{N}^2\rangle-\langle \hat{N}\rangle^2, \tag{6.1}$$

where $\hat{N}$ is the neutron number operator and the expectation values are with respect to the BCS or HFB wave function. For even $Z=N$ nuclei, these wave functions have the form given in Eq. (4.6). It can then be demonstrated that

$$(\Delta N)^2=2\sum_{\alpha>0} u_\alpha^2 v_\alpha^2+2\sum_{\alpha>0} u_\alpha^2 v_{\alpha 2}^2, \tag{6.2}$$

where v_α is given in Eq. (4.7). There are several limiting cases. (1) If there is proton-proton pairing and neutron-neutron pairing, but no proton-neutron pairing, then $v_{\alpha 1}=v_{\alpha 3}=0$ and $v_\alpha=v_{\alpha 2}$, so that

$$(\Delta N)^2=4\sum_{\alpha>0} u_\alpha^2 v_\alpha^2. \tag{6.3}$$

This is the usual result for $p\bar{p}$ and $n\bar{n}$ pairing [79]. (2) If there is proton-neutron pairing, but no proton-proton pairing or neutron-neutron pairing, then $v_{\alpha 2}=0$, so that

$$(\Delta N)^2=2\sum_{\alpha>0} u_\alpha^2 v_\alpha^2. \tag{6.4}$$

Comparing Eqs. (6.3) and (6.4), we obtain the interesting result that the fluctuation in the neutron number $(\Delta N)^2$ is reduced by a factor of 2 if there is only proton-neutron pairing, compared to the case where there is only pairing between like nucleons. This is true even when the neutron orbital occupation probabilities v_α^2 have the same values for both cases. Why does this happen? It is because the fluctuation $(\Delta N)^2$ includes terms such as $\langle C_{\alpha n}^\dagger C_{\bar{\alpha} n}^\dagger\rangle\langle C_{\bar{\alpha} n} C_{\alpha n}\rangle$, which equals $u_\alpha^2 v_{\alpha 2}^2$ if there is $n\bar{n}$ pairing, but this term equals zero if there is no $n\bar{n}$ pairing. (3) If there is $T=0$ pairing, but no $T=1$ pairing, then $v_{\alpha 2}=\mathrm{Re}\, v_{\alpha 3}=0$, so that ΔN is again given by Eq. (6.4). (4) If there is $T=1$ ($p\bar{p},n\bar{n}$ and $p\bar{n}$) pairing, but no $T=0$ pairing, then $v_{\alpha 1}=\mathrm{Im}\, v_{\alpha 3}=0$ and $v_{\alpha 2}=\mathrm{Re}\, v_{\alpha 3}$, so that

TABLE II. Fluctuation in the neutron number ΔN for BCS ground states. Results are given for different choices of the single nucleon energy e_j and $S_p=1.45$.

Nucleus	ΔN^{a}	ΔN^{b}	ΔN^{c}
^{76}Sr	1.55	1.91	1.63
^{80}Zr	1.63	1.55	1.60
^{84}Mo	1.10	0	1.21
^{88}Ru	1.12	0	0
^{92}Pd	1.71	1.02	1.02
^{96}Cd	1.18	1.40	1.59

[a] For $e_j(^{57}$Ni$)$.
[b] For $e_j($Nilsson$)$.
[c] For $e_j($KFP$)$.

$$(\Delta N)^2=3\sum_{\alpha>0} u_\alpha^2 v_\alpha^2. \tag{6.5}$$

The conclusion is that for a given set of neutron orbital occupation probabilities v_α^2, the fluctuation in the neutron number ΔN is largest when there is no proton-neutron pairing. Introducing any type of proton-neutron pairing reduces the fluctuation in neutron number. (Of course, all statements above also apply to fluctuations in the proton number.)

The fluctuation in the neutron number ΔN is given in Table II for the BCS ground states. These values of ΔN are significantly smaller than those usually found for $p\bar{p}$ and $n\bar{n}$ pairing. For $p\bar{p}$ and $n\bar{n}$ pairing, the weak pairing limit gives $\Delta N\simeq\sqrt{6}$, and the strong pairing limit gives $\Delta N=\sqrt{N}$ for a half-filled j shell, where here N is the number of neutrons in the j shell [79]. The even $Z=N$ isotopes considered here have values of Z and N which change in steps of 2. The fluctuations ΔN in Table II are all smaller than 2. Therefore the major component of these wave functions is centered on the isotope of interest, with substantially smaller components from neighboring isotopes.

B. Isospin fluctuations

The nucleon-nucleon strong interaction conserves the isospin T. Do the BCS and HFB wave functions conserve isospin? The isospin vector is

$$\mathbf{T}=T_x\hat{i}+T_y\hat{j}+T_z\hat{k}. \tag{6.6}$$

For even $Z=N$ nuclei, the BCS and HFB wave functions are given by Eq. (4.6). The isospin is block diagonal in the quartets of states $|\alpha p\rangle$, $|\alpha n\rangle$, $|\bar{\alpha} p\rangle$, and $|\bar{\alpha} n\rangle$, and for each quartet its representation is

$$T_m=\frac{1}{2}\begin{pmatrix} \tau_m & 0 \\ 0 & \tau_m \end{pmatrix}, \tag{6.7}$$

where $m=x,y,z$ and τ_m is a 2×2 Pauli spin matrix. The expectation value of an isospin component is

$$\langle T_m\rangle=\mathrm{Tr}(T_m\rho), \tag{6.8}$$

where ρ is the density matrix (5.13). For the wave function (4.6), the density matrix is block diagonal in the quartets of states, and for each quartet

$$\rho = v_\alpha^2 I, \tag{6.9}$$

where v_α is given by Eq. (4.7) and I is the 4×4 unit matrix. Therefore

$$\langle T_m \rangle = 0, \quad \langle \mathbf{T} \rangle = 0. \tag{6.10}$$

The average value of the isospin vector is zero in the BCS and HFB ground state. The fluctuation in $\mathbf{T}$ is

$$(\Delta \mathbf{T})^2 = \langle \mathbf{T} \cdot \mathbf{T} \rangle - \langle \mathbf{T} \rangle \cdot \langle \mathbf{T} \rangle = \langle \mathbf{T} \cdot \mathbf{T} \rangle = \sum_{m=x,y,z} \langle T_m^2 \rangle. \tag{6.11}$$

The isospin component T_m is a one-body operator, and T_m^2 separates into a one-body operator plus a two-body operator. From Wick's theorem it follows that

$$\langle T_m^2 \rangle = \mathrm{Tr}(T_m^2 \rho) + [\mathrm{Tr}(T_m \rho)]^2 - \mathrm{Tr}(T_m \rho)^2 - \mathrm{Tr}(T_m t T_m^* t^*), \tag{6.12}$$

where t is the pairing tensor (5.14). For the wave function (4.6), the pairing tensor is block diagonal in the quartets of states, and for each quartet

$$t = -v^\dagger(\alpha) u(\alpha), \tag{6.13}$$

where the 4×4 matrices $u(\alpha)$ and $v(\alpha)$ are given by Eqs. (4.4) and (4.5). The first term in Eq. (6.12) is obtained from the one-body operator part of T_m^2, while the next three terms are the HF direct, the HF exchange, and the pairing contributions derived from the two-body operator component of T_m^2. From Eqs. (6.8) and (6.10), it follows that the HF direct term equals 0. By substituting Eqs. (6.7), (6.9), and (6.13) into Eq. (6.12), it can be demonstrated that the fluctuation in the isospin is

$$(\Delta \mathbf{T})^2 = 4 \sum_{\alpha>0} u_\alpha^2 v_\alpha^2 - 4 \sum_{\alpha>0} u_\alpha^2 |v_{\alpha 1}|^2 - 4 \sum_{\alpha>0} u_\alpha^2 (\mathrm{Im}\, v_{\alpha 3})^2, \tag{6.14}$$

where u_α and $v_{\alpha i}$ are taken from the wave function (4.6) and v_α is defined in Eq. (4.7). There are several limiting cases. (1) If there is proton-proton pairing and neutron-neutron pairing, but no proton-neutron pairing, then $v_{\alpha 1} = v_{\alpha 3} = 0$, so that

$$(\Delta \mathbf{T})^2 = 4 \sum_{\alpha>0} u_\alpha^2 v_\alpha^2. \tag{6.15}$$

So even when there is no proton-neutron pairing, there is a fluctuation in the isospin. Furthermore the isospin fluctuation equals the neutron number fluctuation (6.3). (2) If there is $T=1$ ($p\bar{p}$, $n\bar{n}$ and $p\bar{n}$) pairing, but no $T=0$ pairing, then $v_{\alpha 1} = \mathrm{Im}\, v_{\alpha 3} = 0$, and Eq. (6.15) is again the result. So introducing $p\bar{n}(T=1)$ pairing causes no change in the isospin

TABLE III. Fluctuation in the isospin $\Delta \mathbf{T}$ for BCS ground states. Results are given for different choices of the single nucleon energy e_j and $S_p = 1.45$.

Nucleus	$\Delta \mathbf{T}^a$	$\Delta \mathbf{T}^b$	$\Delta \mathbf{T}^c$
[76]Sr	1.79	2.21	1.88
[80]Zr	1.88	1.75	1.85
[84]Mo	1.27	0	1.37
[88]Ru	1.07	0	0
[92]Pd	1.73	0	0
[96]Cd	0	1.27	1.83

[a]For $e_j(^{57}\mathrm{Ni})$.
[b]For $e_j(\mathrm{Nilsson})$.
[c]For $e_j(\mathrm{KFP})$.

fluctuation. (3) If there is only $T=0(p\bar{n})$ pairing, then $v_{\alpha 1} = v_{\alpha 2} = \mathrm{Re}\, v_{\alpha 3} = 0$ and $v_\alpha^2 = (\mathrm{Im}\, v_{\alpha 3})^2$, so that

$$(\Delta \mathbf{T})^2 = 0. \tag{6.16}$$

There are no fluctuations in the isospin. Since every nucleon pair is coupled to $T=0$, the BCS and HFB wave functions have good isospin $T=0$, and isospin is conserved. (4) If there is only $T=0(pn)$ pairing, then $v_{\alpha 2} = v_{\alpha 3} = 0$ and $v_\alpha^2 = |v_{\alpha 1}|^2$, and Eq. (6.16) is again obtained. There is no isospin fluctuation. (5) If there is only $T=0$ ($p\bar{n}$ and pn) pairing, then $v_{\alpha 2} = \mathrm{Re}\, v_{\alpha 3} = 0$ and $v_\alpha^2 = |v_{\alpha 1}|^2 + (\mathrm{Im}\, v_{\alpha 3})^2$, and Eq. (6.16) is the result. Isospin is conserved. (6) If there is $T=0$ pairing and $T=1$ pairing, then the isospin fluctuation is intermediate between Eqs. (6.15) and (6.16). (7) If there is no pairing, then HFB reduces to HF, where $u_\alpha = 0$, $v_\alpha = 1$ or $u_\alpha = 1$, $v_\alpha = 0$, and Eq. (6.16) is obtained.

The conclusion is that the isospin fluctuation is largest for the conventional case where there is only proton-proton and neutron-neutron pairing. Introducing proton-neutron pairing does not increase the isospin fluctuation. If there is only $T=0$ proton-neutron pairing, then the isospin fluctuation vanishes, and isospin is conserved.

The fluctuation in the isospin $\Delta \mathbf{T}$ is given in Table III for the BCS ground states. The states with only $T=0$ pairing have $\Delta \mathbf{T}=0$. These include two ^{92}Pd states and one ^{96}Cd state. The other states with $\Delta \mathbf{T}=0$ have no pairing. The states with small, but nonzero, fluctuations have both $T=0$ and $T=1$ pairing. The states with the largest fluctuations have only $T=1$ pairing.

VII. EXPERIMENTAL SIGNATURES OF PROTON-NEUTRON PAIRING

There are several possible ways to experimentally detect the presence of proton-neutron pairing. First, consider the ground states of odd-odd $N=Z$ nuclei. For $A<40$ these isotopes have a $T=0$ ground state. (The one exception is ^{34}Cl.) The last proton and last neutron couple to $T=0$ rather than $T=1$, indicating that the nuclear interaction is stronger in the $T=0$ channel than in the $T=1$ channel. Most notably, the deuteron is bound with $T=0$, whereas the dineutron is not bound. For $A=42$–54 the odd-odd $N=Z$ nuclei have $T=1$

ground states, but ^{58}Cu reverts to $T=0$. There is little experimental information available regarding the isospin of the ground state for odd-odd $N=Z$ nuclei with $A>70$. (One notable exception is ^{74}Rb.) If this could be determined for the $A=76-98$ mass region, it could be compared with the systematics I have calculated for the preferred pair mode in even-even $N=Z$ nuclei in this mass region.

Second, consider pair transfer reactions. They are sensitive to the correlations between the two nucleons which are transferred. The value of the neutron-neutron pair transfer amplitude $\langle A+2|C_n^\dagger C_n^\dagger|A\rangle$ depends upon whether the two neutrons form a correlated Cooper pair, and similarly for two protons. (If the two neutrons are coupled to spin zero, then in the BCS approximation the transfer amplitude is proportional to the pair field Δ [80].) Therefore the proton-neutron pair transfer amplitude $\langle A+2|C_p^\dagger C_n^\dagger|A\rangle$ should measure whether or not the proton and neutron form a correlated Cooper pair. Consequently proton-neutron pair transfer reactions might provide an experimental signature for the existence of proton-neutron pair correlations. At present this data is not available. Future calculations will compare pair transfer rates for wave functions which have proton-neutron pairing, and wave functions where the proton-neutron pairing is omitted. This will show how proton-neutron pairing alters the proton-neutron pair transfer amplitude.

Third, consider the effect of rotation upon pairing. For $p\bar{p}$ and $n\bar{n}$ Cooper pairs, the spins of the two nucleons are anti-parallel. When the nucleus is rotated, the Coriolis force has an opposite effect on each nucleon in the pair. The Coriolis force tends to align both nucleon spins along the rotation axis, which breaks the pair and loses pairing energy. This is the old Coriolis anti-pairing effect. However, for pn Cooper pairs, the spins of the two nucleons are parallel. When the nucleus is rotated, the Coriolis force has the same effect on both nucleons in the pair. For pn pairs rotation aligns both nucleon spins along the rotation axis without breaking the pair or losing pairing energy. There is no Coriolis antipairing effect. This permits the scenario in which a ground state band with $T=1$ pairing is crossed by a band with $T=0$ pairing at a crossing frequency ω_c. This is the scenario proposed for ^{74}Rb [44,50]. If there is a band crossing, how can one determine whether it is a crossing of the ground band with a conventional aligned band (two nucleons aligned along the rotation axis) or whether it is a crossing of two bands having different kinds of Cooper pairs? There are indications that these two types of band crossings correspond to different numerical values for ω_c [58]. Much experimental and theoretical work remains to be done to show more conclusively how different magnitudes for ω_c can distinguish between the two types of band crossings.

Fourth, consider the effect of temperature upon pairing. At a critical temperature T_c the thermal excitations break the Cooper pairs, and the equilibrium value of the pair field Δ vanishes. There is a phase transition from the superfluid phase to the normal phase. At this phase transition there is a peak in the specific heat, which corresponds to a discontinuity in the derivative of the level density with respect to the temperature. Therefore experimental level densities might provide information regarding this pairing phase transition. Calculations [37,38] on ^{24}Mg found that if only $J=0$, $T=1$ Cooper pairs are included, then $T_c=1.5$ MeV. However, if Cooper pairs with all possible values of J and T are included, then $T_c=3.4$ MeV. So the abrupt change in the experimental level density should occur at a temperature which is strongly dependent upon the nature of the Cooper pairs. Fifth, proton-neutron pairing is expected to have a significant effect upon β decay rates [7–9].

VIII. CONCLUSIONS

Pairing correlations have been calculated for the ground states of even $Z=N$ nuclei with $A=76-96$. The isospin generalized BCS equations and the HFB equation have been utilized. These calculations simultaneously include $p\bar{p}$, $n\bar{n}$, $p\bar{n}(T=1)$, $p\bar{n}(T=0)$, and $pn(T=0)$ Cooper pairs, as well as the time-reverse of these proton-neutron pairs. The HFB ground state has the following pairing properties: For all three choices of the single-nucleon energy e_j, there is a transition from $T=1$ pairing at the beginning of this isotope sequence to $T=0$ pairing at the end of the sequence. (The only exception is ^{96}Cd with the KFP choice of e_j, where the $T=1$ pairing state is slightly below the $T=0$ pairing state.) Near the middle of the isotope sequence, the ^{57}Ni and KFP choices of e_j lead to coexistence of a $T=0$ pair superfluid and a $T=1$ pair superfluid. Here the $T=0$ pair phase and the $T=1$ pair phase coexist in the same HFB wave function. The isospin generalized BCS calculations also find this phase coexistence in some isotopes. Consequently $T=0$ Cooper pairs and $T=1$ Cooper pairs are not mutually exclusive in isospin generalized BCS and HFB calculations.

Deformations have been calculated for these isotopes. The various choices for the single-particle energies e_j give different ground state shapes and different prolate-oblate energy separations. This confirms the early finding that the ground state shapes of these isotopes are unusually sensitive to the choice of the parameters in the Hamiltonian [67,72,74].

Fluctuations in the particle number and isospin were considered. Analytic and numerical results demonstrate that for a given set of orbital occupation probabilities v_α^2, the fluctuation in the proton number or neutron number is largest when there is proton-proton pairing and neutron-neutron pairing, but no proton-neutron pairing. If proton-neutron pairing is introduced, then these number fluctuations are reduced, even when the values of v_α^2 are held constant. Similarly, analytic and numerical results show that for given values of v_α^2, the fluctuation in the isospin is largest when there is only proton-proton pairing and neutron-neutron pairing. Introducing $T=1$ proton-neutron pairing does not increase the isospin fluctuation. If there is only $T=0$ proton-neutron pairing, then the isospin fluctuation disappears, and isospin is conserved.

[1] H. Grawe, R. Schubart, K. Maier, and D. Seweryniak, Phys. Scr. **T56**, 71 (1995).

[2] H. Grawe *et al.*, in *Highlights of Modern Nuclear Structure*, Proceedings of the *6th International Spring Seminar on Nuclear Physics*, S. Agata, Italy, 1998, edited by A. Covello (World Scientific, Singapore, 1998).

[3] J. Dobaczewski, I. Hamamoto, W. Nazarewicz, and J. Sheikh, Phys. Rev. Lett. **72**, 981 (1994).

[4] W. Nazarewicz, T. Werner, and J. Dobaczewski, Phys. Rev. C **50**, 2860 (1994).

[5] J. Dobaczewski and W. Nazarewicz, Phys. Rev. C **51**, R1070 (1995).

[6] R. Smolanczuk and J. Dobaczewski, Phys. Rev. C **48**, R2166 (1993).

[7] M. Cheoun, A. Faessler, F. Simkovic, G. Teneva, and A. Bobyk, Nucl. Phys. **A587**, 301 (1995).

[8] G. Pantis, F. Simkovic, J. Vergados, and A. Faessler, Phys. Rev. C **53**, 695 (1996).

[9] F. Iachello, in *Shell Model and Nuclear Structure*, Proceedings of the 2nd International Spring Seminar on Nuclear Physics, Capri, Italy, 1988, edited by A. Covello (World Scientific, Singapore, 1989) p. 407.

[10] A. Bohr, B. Mottelson, and D. Pines, Phys. Rev. **110**, 936 (1958).

[11] S. Belyaev, Mat. Fys. Medd. K. Dan. Videusk. Selsk. **31**, No. 11 (1959).

[12] A. M. Lane, *Nuclear Theory* (Benjamin, New York, 1964), Chap. 5-1.

[13] A. L. Goodman, Adv. Nucl. Phys. **11**, 263 (1979).

[14] A. Goswami, Nucl. Phys. **60**, 228 (1964).

[15] A. Goswami and L. Kisslinger, Phys. Rev. **140**, B26 (1965).

[16] P. Camiz, A. Covello, and M. Jean, Nuovo Cimento **36**, 663 (1965).

[17] P. Camiz, A. Covello, and M. Jean, Nuovo Cimento B **42**, 199 (1966).

[18] H. Chen and A. Goswami, Phys. Lett. **24B**, 257 (1967).

[19] A. Goodman, G. Struble, and A. Goswami, Phys. Lett. **26B**, 260 (1968).

[20] A. Goodman, Ph.D. thesis, Berkeley, Report No. UCLRL-19514, 1969.

[21] J. Bar-Touv, A. Goswami, A. Goodman, and G. Struble, Phys. Rev. **178**, 1670 (1969).

[22] A. Goodman, G. Struble, J. Bar-Touv, and A. Goswami, Phys. Rev. C **2**, 380 (1970).

[23] A. Goodman, Nucl. Phys. **A186**, 475 (1972).

[24] H. Wolter, A. Faessler, and P. Sauer, Phys. Lett. **31B**, 516 (1970).

[25] H. Wolter, A. Faessler, and P. Sauer, Nucl. Phys. **A167**, 108 (1971).

[26] K. Goeke, A. Faessler, and H. Wolter, Nucl. Phys. **A183**, 352 (1972).

[27] K. Goeke, J. Garcia, and A. Faessler, Nucl. Phys. **A208**, 477 (1973).

[28] T. Sandhu, M. Rustgi, and A. Goodman, Phys. Rev. C **12**, 1340 (1975).

[29] P. Mpanias and M. Rustgi, Phys. Rev. C **14**, 365 (1976).

[30] T. Sandhu and M. Rustgi, Phys. Rev. C **14**, 675 (1976).

[31] K. Nichols and R. Sorensen, Nucl. Phys. **A309**, 45 (1978).

[32] K. Muhlhans, E. Muller, K. Neergard, and U. Mosel, Phys. Lett. **105B**, 329 (1981).

[33] E. Muller, K. Muhlhans, K. Neergard, and U. Mosel, Nucl. Phys. **A383**, 233 (1982).

[34] A. L. Goodman, Nucl. Phys. **A352**, 30 (1981).

[35] K. Tanabe, K. Sugawara-Tanabe, and H. J. Mang, Nucl. Phys. **A357**, 20 (1981).

[36] A. Goodman, Nucl. Phys. **A402**, 189 (1983).

[37] K. Muhlhans, E. Muller, U. Mosel, and A. Goodman, Z. Phys. A **313**, 133 (1983).

[38] K. Muhlhans, U. Mosel, K. Neergard, M. Diebel, E. Muller, and A. Goodman, Proceedings of the International Meeting on Nuclear Physics, Bormio, 1983 (unpublished).

[39] M. Mukerjee, Phys. Lett. B **297**, 1 (1992).

[40] R. Page *et al.*, Phys. Rev. Lett. **72**, 1798 (1994).

[41] S. Frauendorf, J. Sheikh, and N. Rowley, Phys. Rev. C **50**, 196 (1994).

[42] S. Frauendorf and J. Sheikh, Phys. Rev. C **59**, 1400 (1999).

[43] A. Petrovici, K. Schmid, and A. Faessler, Nucl. Phys. **A605**, 290 (1996).

[44] D. Rudolph *et al.*, Phys. Rev. Lett. **76**, 376 (1996).

[45] C. Gross *et al.*, Phys. Rev. C **56**, R591 (1997).

[46] J. Uusitalo *et al.*, Phys. Rev. C **57**, 2259 (1998).

[47] D. Dean, S. Koonin, K. Langanke, P. Radha, and Y. Alhassid, Phys. Rev. Lett. **74**, 2909 (1995).

[48] K. Langanke, D. Dean, P. Radha, and S. Koonin, Nucl. Phys. **A602**, 244 (1996).

[49] K. Langanke, D. Dean, S. Koonin, and P. Radha, Nucl. Phys. **A613**, 253 (1997).

[50] D. Dean, S. Koonin, K. Langanke, and P. Radha, Phys. Lett. B **399**, 1 (1997).

[51] J. Engel, K. Langanke, and P. Vogel, Phys. Lett. B **389**, 211 (1996).

[52] J. Engel, S. Pittel, M. Stoitsov, P. Vogel, and J. Dukelsky, Phys. Rev. C **55**, 1781 (1997).

[53] J. Dobes and S. Pittel, Phys. Rev. C **57**, 688 (1998).

[54] O. Civitarese and M. Reboiro, Phys. Rev. C **56**, 1179 (1997).

[55] O. Civitarese, M. Reboiro, and P. Vogel, Phys. Rev. C **56**, 1840 (1997).

[56] W. Satula and R. Wyss, Phys. Lett. B **393**, 1 (1997).

[57] J. Terasaki, R. Wyss, and P. Heenen, Phys. Lett. B **437**, 1 (1998).

[58] K. Kaneko and J. Zhang, Phys. Rev. C **57**, 1732 (1998).

[59] A. Sedrakian, T. Alm, and U. Lombardo, Phys. Rev. C **55**, R582 (1997).

[60] P. Van Isacker and D. Warner, Phys. Rev. Lett. **78**, 3266 (1997).

[61] E. Kirchuk, P. Federman, and S. Pittel, Phys. Rev. C **47**, 567 (1993).

[62] A. Nowacki, Ph.D. thesis, Madrid, Spain, 1995.

[63] D. Bucurescu *et al.*, Rev. Roum. Phys. **24**, 971 (1979).

[64] P. Moller and R. Nix, Nucl. Phys. **A361**, 117 (1981).

[65] P. Moller and R. Nix, At. Data Nucl. Data Tables **26**, 165 (1981).

[66] S. Aberg, Phys. Scr. **25**, 23 (1982).

[67] K. Heyde, J. Moreau, and M. Waroquier, Phys. Rev. C **29**, 1859 (1984).

[68] P. Bonche, H. Flocard, P. Heenen, S. Krieger, and M. Weiss, Nucl. Phys. **A443**, 39 (1985).

[69] W. Nazarewicz, J. Dudek, R. Bengtsson, T. Bengtsson, and I. Ragnarsson, Nucl. Phys. **A435**, 397 (1985).

[70] D. Ahalpara, K. Bhatt, and A. Abzouzi, Nucl. Phys. **A445**, 1 (1985).

[71] S. Aberg, H. Flocard, and W. Nazarewicz, Annu. Rev. Nucl. Part. Sci. **40**, 439 (1990).

[72] C. Lister, *et al.* Phys. Rev. Lett. **59**, 1270 (1987).

[73] U. Huttmeier *et al.*, Phys. Rev. C **37**, 118 (1988).

[74] C. Lister *et al.*, Phys. Rev. C **42**, R1191 (1990).

[75] W. Gelletly *et al.*, Phys. Lett. B **253**, 287 (1991).

[76] D. Bucurescu *et al.*, Phys. Rev. C **56**, 2497 (1997).

[77] A. Bohr and B. Mottelson, *Nuclear Structure* (Benjamin, New York, 1969) Vol. 1, p. 169.

[78] R. Firestone *et al.*, *Table of Isotopes*, 8th ed. (Wiley, New York, 1996).

[79] P. Ring and P. Schuck, *The Nuclear Many-Body Problem* (Springer-Verlag, New York, 1980), pp. 230, 242.

[80] R. Nikam, P. Ring, and L. Canto, Phys. Lett. B **185**, 269 (1987).